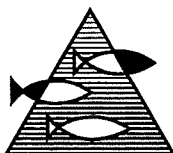


PROSJEKTRAPPORT

ISSN 0071-5638



HAVFORSKNINGSINSTITUTTET

MILJØ - RESSURS - HAVBRUK

Nordnesparken 2 Postboks 1870 5024 Bergen

Tlf.: 55 23 85 00 Faks: 55 23 85 31

Forskningsstasjonen

Flødevigen

4817 His

Tlf.: 37 05 90 00

Faks: 37 05 90 01

Austevoll

Havbruksstasjon

5392 Storebø

Tlf.: 56 18 03 42

Faks: 56 18 03 98

Matre

Havbruksstasjon

5198 Matredal

Tlf.: 56 36 60 40

Faks: 56 36 61 43

Distribusjon:

ÅPEN

HI-prosjektnr.:

Oppdragsgiver(e):

Oppdragsgivers referanse:

Rapport:

FISKEN OG HAVET

NR. 16 - 1998

Tittel:

A SENSITIVITY STUDY OF A BAROCLINIC MODEL
FOR THE NORTH SEA WITH FOCUS ON THE
UTSIRA-ORKNEYS TRANSECT

Senter:

Miljø

Seksjon:

Fysisk oseanografi

Forfatter(e):

Jarle Berntsen

Antall sider, vedlegg inkl.:

48

Dato:

15.10.98

Sammendrag:

Numeriske modeller for beregning av sirkulasjon og hydrografi blir nå benyttet i en rekke viktige studier for våre havområder. I dette arbeidet blir en ny tids-splittet sigmakoordinat havmodell presentert.

Modellen er satt opp på en utvidet Nordsjø med 20 km horisontal oppløsning og følsomhet til modellen overfor valg av parametre er studert. I studiene er data fra gjentatte tokt langs Utsira-Orknøyene-snittet benyttet til validering av modellresultat.

Det er vist at med 20 km horisontal oppløsning er resultatene robuste overfor valg av tidskritt, opp til 1 times 3-D steg kan benyttes, og ovenfor vertikal oppløsning, 11 - 21 lag er tilstrekkelig.

Resultatene er svært følsomme for parametrisering av sub-grid skala effekter. Høyere oppløsning i frontområdet er antagelig påkrevet for å få effektene av småskala hvirvler riktig representert på stor skala sirkulasjon.

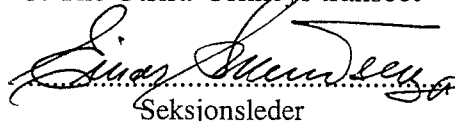
Emneord - norsk:

1. Numerisk havmodell
2. Sensitivitetsstudier
3. Utsira-Orknøyene-snittet


Prosjektleder

Emneord - engelsk:

1. Numerical ocean model
2. Sensitivity studies
3. The Utsira-Orkneys transect


Seksjonsleder

k 5598

A sensitivity study of a baroclinic model for the North Sea with focus on the Utsira-Orkneys transect

Jarle Berntsen¹

Department of Mathematics

University of Bergen

Johs. Bruns gt. 12, N-5008 Bergen

and

Institute of Marine Research

Nordnesparken 2, N-5024 Bergen,

October 1998

Abstract

The purpose of the present report is to study the sensitivity of a numerical time split σ -coordinate ocean model for the North Sea with 20 km horizontal resolution to sub grid scale parametrizations, the vertical resolution and the time step. Measurements of salinity across the Utsira-Orkneys transect taken from 1972 to 1996 are compared to model results.

It is demonstrated that both the residual transports and the models salinity and density structures are very sensitive to the parametrizations of horizontal viscosity and diffusivity in a 20 km resolution baroclinic North Sea model. The sensitivity is strongly related to smaller scale baroclinic instabilities not resolved by the model. These eddies are of major importance for the creation of also the larger scale density structures along the Norwegian coast. Evidence is given to support the hypothesis that the larger scale fields may not be correctly reproduced by choosing appropriate parametrizations. In a 20 km resolution baroclinic North Sea model it is sufficient with between 10 and 20 σ -layers in the vertical. The present time split σ -coordinate 20 km North Sea model is robust to the choice of time step. 1 hour 3-D steps may be applied without any major degradation of the quality of the output.

Keywords: regional circulation models, stratified oceans, parametrizations of sub grid scale processes, vertical resolution, time steps, the North Sea, the Utsira-Orkneys transect

¹Author, email: jarle.berntsen@mi.uib.no, fax: 47-55-589672

1 Introduction.

Numerical ocean models for the North Sea are now applied in numerous studies. The horizontal resolution in many 3-D studies is still approximately 20km, see for instance Smith *et al.* [23] or Engedahl *et al.* [13], either for the whole domain or for a larger scale domain providing initial and boundary values for a finer scale domain covering a smaller part of the ocean, see for instance Svendsen *et al.* [25].

In the present paper observations of salinity across the Utsira-Orkneys transect taken from 1972 to 1996 and estimates of residual transports are used to study the sensitivity of a numerical time split σ -coordinate ocean model for the North Sea with 20 km horizontal resolution to sub grid scale parametrizations, the vertical resolution and the time step.

The model is run from 15/10-89 to 15/11-89 and forced with climatological values through the open boundaries, 4 components of the tide, atmospheric forcing and mean river runoff from the major rivers. The model equations are given in section 3. The numerical time split σ -coordinate model is described in section 3. In section 4 the specifics for the North Sea experiments are given. Data from measurements across the Utsira-Orkneys transect are presented in section 5 and comparisons with the climatology are found in section 6. In sections 7, 8, 9 and 10 the sensitivity to the vertical resolution, the horizontal viscosity formulation, the horizontal diffusivity and the time step is studied. A discussion of the findings is given in section 11 and the major conclusions are summarized in section 12.

2 The model equations

The physical variables and governing equations for these are given in Berntsen *et al.* [5]. For completeness the equations are repeated below.

$$\nabla \cdot \vec{U} + \frac{\partial W}{\partial z} = 0, \quad (1)$$

$$\frac{\partial U}{\partial t} + \vec{U} \cdot \nabla U + W \frac{\partial U}{\partial z} - fV = -\frac{1}{\rho_0} \frac{\partial P}{\partial x} + \frac{\partial}{\partial z} (K_M \frac{\partial U}{\partial z}) + F_x, \quad (2)$$

$$\frac{\partial V}{\partial t} + \vec{U} \cdot \nabla V + W \frac{\partial V}{\partial z} + fU = -\frac{1}{\rho_0} \frac{\partial P}{\partial y} + \frac{\partial}{\partial z} (K_M \frac{\partial V}{\partial z}) + F_y, \quad (3)$$

$$P = P_{atm} + g\rho_0\eta + g \int_z^0 \rho(z') dz', \quad (4)$$

$$\frac{\partial T}{\partial t} + \vec{U} \cdot \nabla T + W \frac{\partial T}{\partial z} = \frac{\partial}{\partial z} (K_H \frac{\partial T}{\partial z}), \quad (5)$$

$$\frac{\partial S}{\partial t} + \vec{U} \cdot \nabla S + W \frac{\partial S}{\partial z} = \frac{\partial}{\partial z} (K_H \frac{\partial S}{\partial z}). \quad (6)$$

In the present study we have regarded it to be sufficient to apply a simplified equation of state of the form

$$\rho = \rho(T, S) \quad (7)$$

taken from [28] instead of the UNESCO equation of state [27]. In the equations above $\vec{U} = (U, V)$ are horizontal velocities in x - and y -direction respectively, W the vertical velocity, η the surface elevation, P the in-situ pressure, P_{atm} the atmospheric pressure, ρ the density, $\rho_0 = 1025.0 \text{ kg m}^{-3}$ the reference density, S salinity, T temperature, K_M vertical eddy viscosity, A_M horizontal eddy viscosity, K_H vertical eddy diffusivity, $g = 9.81 \text{ m s}^{-2}$ the gravity constant and $f = 1.3 \times 10^{-4} \text{ s}^{-1}$ the Coriolis parameter.

The Mellor and Yamada 2 1/2 level model with the Galperin *et al.* modifications is applied to compute K_M and K_H . The governing equations in z -coordinates for turbulent kinetic energy, $q^2/2$, and turbulent macro scale, l , are given below, see [15, 18],

$$\frac{\partial q^2}{\partial t} = \frac{\partial}{\partial z} \left(K_q \frac{\partial q^2}{\partial z} \right) + 2K_M \left[\left(\frac{\partial U}{\partial z} \right)^2 + \left(\frac{\partial V}{\partial z} \right)^2 \right] + \frac{2g}{\rho_0} K_H \frac{\partial \rho}{\partial z} - \frac{2q^3}{B_1 l}$$

$$\frac{\partial q^2 l}{\partial t} = \frac{\partial}{\partial z} \left(K_q \frac{\partial q^2 l}{\partial z} \right) + l E_1 K_M \left[\left(\frac{\partial U}{\partial z} \right)^2 + \left(\frac{\partial V}{\partial z} \right)^2 \right] + \frac{l E_1 g}{\rho_0} K_H \frac{\partial \rho}{\partial z} - \frac{q^3}{B_1} \tilde{W}$$

where

$$\tilde{W} = 1 + E_2 \left(\frac{l}{\kappa L} \right)^2 \quad (8)$$

and where

$$L^{-1} = (\eta - z)^{-1} + (H + z)^{-1}. \quad (9)$$

$\kappa = 0.4$ is the von Karman constant. Based on scaling arguments advection of q^2 and $q^2 l$ is neglected. Defining

$$G_H = \frac{l^2}{q^2} \frac{g}{\rho_0} \frac{\partial \rho}{\partial z} \quad (10)$$

the stability functions become

$$S_H [1 - (3A_2 B_2 + 18A_1 A_2) G_H] = A_2 [1 - 6A_1 / B_1] \quad (11)$$

and

$$S_M [1 - 9A_1 A_2 G_H] - S_H [18A_1^2 + 9A_1 A_2] G_H = A_1 [1 - 3C_1 - 6A_1 / B_1] \quad (12)$$

K_M , K_H and K_q are then computed according to

$$K_M = l q S_M \quad (13)$$

$$K_H = l q S_H \quad (14)$$

$$K_q = 0.20 l q \quad (15)$$

The empirical values in the expressions above are

$$(A_1, A_2, B_1, B_2, C_1, E_1, E_2) = (0.92, 0.74, 16.6, 10.1, 0.08, 1.8, 1.33) \quad (16)$$

In practice it is customary to apply lower limits for K_M and K_H and the quality of the numerical outputs may depend on the choice of these limits, see for instance Berntsen and Svendsen [6]. In the present experiments the minimum allowed value for K_M is $1 \times 10^{-5} m^2 s^{-1}$ and for K_H $1 \times 10^{-7} m^2 s^{-1}$.

2.1 The horizontal viscosities

The horizontal viscous terms F_x and F_y are written in the form:

$$F = \frac{\partial}{\partial x} \left(A_M \frac{\partial F}{\partial x} \right) + \frac{\partial}{\partial y} \left(A_M \frac{\partial F}{\partial y} \right). \quad (17)$$

The horizontal viscosity, A_M , is computed according to Smagorinsky [22]

$$A_M = C_M \Delta x \Delta y \frac{1}{2} \left[\left(\frac{\partial U}{\partial x} \right)^2 + \frac{1}{2} \left(\frac{\partial V}{\partial x} + \frac{\partial U}{\partial y} \right)^2 + \left(\frac{\partial V}{\partial y} \right)^2 \right]^{\frac{1}{2}}, \quad (18)$$

where Δx and Δy are the grid spacing in x -direction and y -direction respectively. The horizontal viscosity coefficient, C_M , is chosen to be 1.0 in our experiments. In the studies of effects vertical resolution and horizontal viscosity (sections 7 and 8) the horizontal diffusivity terms are neglected as in equations (5) and (6). In the studies of effects of horizontal diffusivity and the time step the diffusivity terms in the form (17) are added to the equations (5) and (6) and the diffusivities A_H are chosen to be equal to A_M .

To run the model to be described with this formulation for A_M suffices to get stable simulations. However, as will be demonstrated, small scale oscillations tend to create excessive down- and up-welling in the Norwegian Coastal Current (NCC) and unrealistic density profiles across the NCC. Our interpretation of this is that with the present horizontal resolution, 20km, the internal Rossby radius for this area, from 1 to 10km approximately, is far from resolved and instabilities on Rossby radius scale is therefore misrepresented or aliased at the $2\Delta x$ scale and creates convergence and divergence and unrealistically large vertical velocities. In experiments from this area, see Berntsen and Svendsen [6], with finer grid resolution we have not experienced the problem with excessive up- and down-welling and this support the above hypothesis.

For models based on the leapfrog method one may apply an Asselin filter [3] to remove the small scale energy in time and space. This is the strategy applied in the Blumberg and Mellor model [7]. For one step methods time filtering will create phase errors and may not be an acceptable strategy. An alternative is to enhance the horizontal viscosities in cases when the small scale oscillations in the vertical velocities become large. The details for this formulations are specific for the numerical method and described in the next section.

2.2 Boundary conditions

At the surface the following boundary conditions are used

$$\rho_0 K_M \left(\frac{\partial U}{\partial z}, \frac{\partial V}{\partial z} \right) = (\tau_{0x}, \tau_{0y}) \quad (19)$$

$$\rho_0 K_H \frac{\partial S}{\partial z} = 0 \quad (20)$$

$$K_H \frac{\partial T}{\partial z} = \gamma(T^* - T(0)) \quad (21)$$

$$q^2 = B_1^{2/3} u_{\tau_s}^2 \quad (22)$$

$$l = 0.0 \quad (23)$$

where (τ_{0x}, τ_{0y}) is the surface wind stress vector and u_{τ_s} is the magnitude of the vector. To compute the surface heat flux a method of relaxation towards climatology due to Cox and Bryan [8] is used. T^* is the climatological value of the sea surface temperature, $T(0)$ is the models surface temperature and γ a time constant that is selected to be $1.736 \times 10^{-5} m s^{-1}$.

At the bottom the following boundary conditions are used

$$\rho_0 K_M \left(\frac{\partial U}{\partial z}, \frac{\partial V}{\partial z} \right) = (\tau_{bx}, \tau_{by}) \quad (24)$$

$$\rho_0 K_H \frac{\partial S}{\partial z} = 0 \quad (25)$$

$$K_H \frac{\partial T}{\partial z} = 0 \quad (26)$$

$$q^2 = B_1^{2/3} u_{\tau_b}^2 \quad (27)$$

$$l = 0 \quad (28)$$

where (τ_{bx}, τ_{by}) is the bottom frictional stress and u_{τ_b} the friction velocity associ-

ated with the bottom stress

$$\vec{\tau}_b = \rho_0 C_D |\vec{U}_b| \vec{U}_b \quad (29)$$

where the drag coefficient C_D is given by

$$C_D = \max\left[0.0025, \frac{\kappa^2}{(\ln(z_b/z_0))^2}\right] \quad (30)$$

and z_b is the distance of the nearest grid point to the bottom. The von Karman constant $\kappa = 0.4$. In lack of further information we use $z_0 = 0.01m$ for the bottom roughness parameter, see Weatherly and Martin [29].

There are no volume fluxes through the side walls. We also assume a slip conditions at the closed lateral boundaries. On the side walls and bottom of the basin there are no advective or diffusive heat and salt fluxes. The vertical velocities at the free surface and at the bottom are given by

$$W_0 = U \frac{\partial \eta}{\partial x} + V \frac{\partial \eta}{\partial y} + \frac{\partial \eta}{\partial t}, \quad (31)$$

$$W_b = -U_b \frac{\partial H}{\partial x} - V_b \frac{\partial H}{\partial y}. \quad (32)$$

3 The time splitted σ -coordinate model

3.1 The σ -coordinate system

The basic equations have been transformed into a bottom following sigma coordinate system [19]. The independent variables (x, y, z, t) are transformed to (x^*, y^*, σ, t^*) , where

$$x^* = x \quad y^* = y \quad \sigma = \frac{z - \eta}{H + \eta} \quad t^* = t. \quad (33)$$

σ ranges from $\sigma = 0$ at $z = \eta$ to $\sigma = -1$ at $z = -H(x, y)$. Introducing the total depth, $D \equiv H + \eta$, the basic equations may now be written as (after deletion of the asterisks)

$$\frac{\partial UD}{\partial x} + \frac{\partial VD}{\partial y} + \frac{\partial \omega}{\partial \sigma} + \frac{\partial \eta}{\partial t} = 0 \quad (34)$$

where ω is the new vertical velocity. The momentum equations on flux form become

$$\begin{aligned} \frac{\partial UD}{\partial t} + \frac{\partial U^2 D}{\partial x} + \frac{\partial UV D}{\partial y} + \frac{\partial U \omega}{\partial \sigma} - fVD + \frac{D}{\rho_0} \frac{\partial P_{atm}}{\partial x} + gD \frac{\partial \eta}{\partial x} = \\ \frac{\partial}{\partial \sigma} \left(\frac{K_M}{D} \frac{\partial U}{\partial \sigma} \right) - \frac{gD^2}{\rho_0} \int_{\sigma}^0 \left(\frac{\partial \rho}{\partial x} - \frac{\sigma}{D} \frac{\partial D}{\partial x} \frac{\partial \rho}{\partial \sigma} \right) d\sigma + DF_x, \end{aligned} \quad (35)$$

$$\begin{aligned} \frac{\partial VD}{\partial t} + \frac{\partial UV D}{\partial x} + \frac{\partial V^2 D}{\partial y} + \frac{\partial V \omega}{\partial \sigma} + fUD + \frac{D}{\rho_0} \frac{\partial P_{atm}}{\partial y} + gD \frac{\partial \eta}{\partial y} = \\ \frac{\partial}{\partial \sigma} \left(\frac{K_M}{D} \frac{\partial V}{\partial \sigma} \right) - \frac{gD^2}{\rho_0} \int_{\sigma}^0 \left(\frac{\partial \rho}{\partial y} - \frac{\sigma}{D} \frac{\partial D}{\partial y} \frac{\partial \rho}{\partial \sigma} \right) d\sigma + DF_y. \end{aligned} \quad (36)$$

The new conservation equations take the form

$$\frac{\partial TD}{\partial t} + \frac{\partial TUD}{\partial x} + \frac{\partial TVD}{\partial y} + \frac{\partial T\omega}{\partial \sigma} = \frac{\partial}{\partial \sigma} \left(\frac{K_H}{D} \frac{\partial T}{\partial \sigma} \right), \quad (37)$$

$$\frac{\partial SD}{\partial t} + \frac{\partial SUD}{\partial x} + \frac{\partial SV D}{\partial y} + \frac{\partial S\omega}{\partial \sigma} = \frac{\partial}{\partial \sigma} \left(\frac{K_H}{D} \frac{\partial S}{\partial \sigma} \right), \quad (38)$$

and the horizontal viscosity terms are now defined according to

$$DF_x = \frac{\partial}{\partial x} \left(A_M \frac{\partial UD}{\partial x} \right) + \frac{\partial}{\partial y} \left(A_M \frac{\partial UD}{\partial y} \right), \quad (39)$$

$$DF_y = \frac{\partial}{\partial y} \left(A_M \frac{\partial VD}{\partial y} \right) + \frac{\partial}{\partial x} \left(A_M \frac{\partial VD}{\partial x} \right). \quad (40)$$

3.1.1 Vertical boundary conditions

The new boundary conditions for the vertical velocity, ω , in equation (34) become

$$\omega(0) = \omega(-1) = 0. \quad (41)$$

The new conditions at the surface ($\sigma = 0$) becomes

$$\frac{K_M}{D} \left(\frac{\partial U}{\partial \sigma}, \frac{\partial V}{\partial \sigma} \right) = \frac{1}{\rho_0} (\tau_{0x}, \tau_{0y}), \quad (42)$$

$$\frac{K_H}{D} \left(\frac{\partial T}{\partial \sigma}, \frac{\partial S}{\partial \sigma} \right) = (\dot{T}_0, \dot{S}_0), \quad (43)$$

and at the bottom ($\sigma = -1$) the boundary conditions become

$$\frac{K_M}{D} \left(\frac{\partial U}{\partial \sigma}, \frac{\partial V}{\partial \sigma} \right) = \frac{1}{\rho_0} (\tau_{bx}, \tau_{by}), \quad (44)$$

$$\frac{K_H}{D} \left(\frac{\partial T}{\partial \sigma}, \frac{\partial S}{\partial \sigma} \right) = 0. \quad (45)$$

3.2 The methods

The σ -coordinate model applied in the present study is a time splitted version of the model presented in [5]. An Arakawa C-grid is still applied. In each 3-D time step of the model the following actions are taken in the order given:

a) In `internal.f90`: Estimates of the internal pressure terms

$$-\frac{gD^2}{\rho_0} \int_{\sigma}^0 \left(\frac{\partial \rho}{\partial x} - \frac{\sigma}{D} \frac{\partial D}{\partial x} \frac{\partial \rho}{\partial \sigma} \right) d\sigma \quad (46)$$

and

$$-\frac{gD^2}{\rho_0} \int_{\sigma}^0 \left(\frac{\partial \rho}{\partial y} - \frac{\sigma}{D} \frac{\partial D}{\partial y} \frac{\partial \rho}{\partial \sigma} \right) d\sigma \quad (47)$$

are computed and saved in ΔU and ΔV . The method is based on central differences in the σ -coordinate system.

b) In `laxwuv.f90`: Estimates of the non linear terms in the moment equations

$$\frac{\partial U^2 D}{\partial x} + \frac{\partial UV D}{\partial y} + \frac{\partial U \omega}{\partial \sigma} \quad (48)$$

and

$$\frac{\partial UV D}{\partial x} + \frac{\partial V^2 D}{\partial y} + \frac{\partial V \omega}{\partial \sigma} \quad (49)$$

are computed with a second order Lax-Wendroff method and subtracted from the contributions ΔU and ΔV from the internal pressure terms.

c) In `fbcor2d.f90`: The 3-D velocity field is split into its baroclinic part and its depth integrated part according to:

$$(U(x, y, \sigma), V(x, y, \sigma)) = (U_A(x, y) + U_B(x, y, \sigma), V_A(x, y) + V_B(x, y, \sigma)) \quad (50)$$

where

$$(U_A(x, y), V_A(x, y)) = (\int_{-1}^0 U(x, y, \sigma) d\sigma, \int_{-1}^0 V(x, y, \sigma) d\sigma).$$

Depth integrating the moment equations (neglecting for a moment the atmospheric pressure terms) and the continuity equation gives:

$$\frac{\partial U_A D}{\partial x} + \frac{\partial V_A D}{\partial y} + \frac{\partial \eta}{\partial t} = 0, \quad (51)$$

$$\begin{aligned} \frac{\partial U_A D}{\partial t} - f V_A D + g D \frac{\partial \eta}{\partial x} = \\ \frac{\partial}{\partial x} (A_{M2D} \frac{\partial U_A D}{\partial x}) + \frac{\partial}{\partial y} (A_{M2D} \frac{\partial U_A D}{\partial y}) + \frac{1}{\rho_0} (\tau_{0x} - \tau_{bx}) + A_x \end{aligned} \quad (52)$$

and

$$\begin{aligned} \frac{\partial V_A D}{\partial t} + f U_A D + g D \frac{\partial \eta}{\partial y} = \\ \frac{\partial}{\partial y} (A_{M2D} \frac{\partial V_A D}{\partial y}) + \frac{\partial}{\partial x} (A_{M2D} \frac{\partial V_A D}{\partial x}) + \frac{1}{\rho_0} (\tau_{0y} - \tau_{by}) + A_y. \end{aligned} \quad (53)$$

where

$$(A_x, A_y) = \left(\int_{-1}^0 \Delta U d\sigma, \int_{-1}^0 \Delta V d\sigma \right).$$

The horizontal viscosities A_{M2D} are for each time step computed according to equation (18) where (U, V) is replaced by (U_A, V_A) .

For each 3-D time step the 2-D system of equations is stepped forward in time with N2D time steps with time steps $DTE = DT/N2D$ when DT is the 3D time step. In each 2D time step $V_A D$ in each U -point is averaged from the 4 neighboring points with equal weights. Contributions to the U_A -equation from the horizontal viscous terms, the Coriolis term, the bottom and surface stresses, the pressure term and A_x using values of U_A , V_A and η at the present time step. Then U_A is estimated on the next time level with an explicit method. The same procedure is applied for the V_A -equation. Using the values of U_A and V_A at the new time step, (51) is then used to estimate η at the new time step. This is often referred to as the Forward-Backward method. The method is stable as long as the 2-D time step is less or equal to $\frac{\Delta x}{\sqrt{2gD}}$ with D equal to the maximum depth within the model area. In every second time step the V_A -equation is propagated before the U_A -equation. The time splitting applied is very similar to the splitting applied by Slagstad [21] and described later in [1].

The equations for the baroclinic fields U_B and V_B become after subtracting (52) from (35) and (53) from (36) :

$$\begin{aligned} \frac{\partial U_B D}{\partial t} - f V_B D + \frac{1}{\rho_0}(\tau_{0x} - \tau_{bx}) + A_x = \\ \frac{\partial}{\partial x} \left(A_M \frac{\partial U_B D}{\partial x} \right) + \frac{\partial}{\partial y} \left(A_M \frac{\partial U_B D}{\partial y} \right) + \frac{\partial}{\partial \sigma} \left(\frac{K_M}{D} \frac{\partial U_B}{\partial \sigma} \right) + \Delta U \end{aligned} \quad (54)$$

and

$$\begin{aligned} \frac{\partial V_B D}{\partial t} + f U_B D + \frac{1}{\rho_0}(\tau_{0y} - \tau_{by}) + A_y = \\ \frac{\partial}{\partial y} \left(A_M \frac{\partial V_B D}{\partial y} \right) + \frac{\partial}{\partial x} \left(A_M \frac{\partial V_B D}{\partial x} \right) + \frac{\partial}{\partial \sigma} \left(\frac{K_M}{D} \frac{\partial V_B}{\partial \sigma} \right) + \Delta V. \end{aligned} \quad (55)$$

After propagating the 2-D equations N2D time steps with steplength $DT/N2D$ the equations for U_B and V_B are propagated one step with step length DT . The Coriolis terms in U and V points are approximated with equal weight averaging. The horizontal viscosity terms are approximated with central differences. The solutions including all terms except the vertical viscosity terms are stepped forward in time using an explicit method. To avoid unacceptable time step limitations the subsets of the equations involving the vertical viscosity terms are stepped forward in time using a fully implicit method.

After the 3-D time step for U_B and V_B , U and V at the new time step are computed from (50). The σ -coordinate velocities, ω , are computed from (34) using the boundary conditions $\omega(0) = \omega(-1) = 0$.

d) In `atmosph.f90`: If we want to include the effects of gradients in the atmospheric pressure, the gradients are approximated with central differences and U and V are updated with an explicit method for these terms.

After steps a), b), c) and d) the effects of all terms of the equations (34), (35) and (36) are accounted for.

e) In `superbeef.f90`: The scalar fields S and T , or any other scalar field, are advected with a gradient preserving and monotonic advection scheme due to Roe and Sweby [26]. This scheme performed favorably in a comparison due to Yang and Przekwas [30].

f) In `my2halv.f90`: The vertical viscosities and diffusivities are updated with the Mellor and Yamada 2 1/2 scheme.

g) In vertdiff.f90: The scalar fields S and T , are mixed vertically with a fully implicit method.

After the steps e), f) and g) the effects of all terms of the equations (37) and (38) are accounted for.

3.2.1 Horizontal viscosities - 2

From fbcor2d.f90 the routine smagor.f90 is called for each time step. smagor.f90 approximates A_M at the center of each grid cell with centered differences equation (18). That is: A_{Mijk} is computed for all cells (i, j, k) . As discussed in section 2.1, the horizontal gradients of the z -coordinate velocities W may also be chosen to affect the horizontal viscosities and the following formulation is chosen:

$$\begin{aligned} WT_{ijk} &= C_{M2} \Delta x \Delta y (|W_{ijk} - W_{i-1jk}| + |W_{ijk} - W_{i+1jk}| + \\ &\quad |W_{ijk} - W_{ij-1k}| + |W_{ijk} - W_{ij+1k}|) \\ WT_{ijk} &= WT_{i,j,k} * DZ(k) / DZ(KB/2), \quad \text{for } k \leq KB/2, \end{aligned}$$

where C_{M2} is a scaling parameter chosen to be 10.0 in the present experiments unless otherwise stated, $DZ(k)$ the thickness of σ -coordinate layer k , and KB the number of σ -coordinate layer interfaces. The layers of the σ -coordinate model are in the present experiments thinner near the surface, and the second statement above will give larger values of WT near the surface. After the computation of A_{Mijk} and WT_{ijk} for all grid points we select $A_{Mijk} = \max(A_{Mijk}, WT_{ijk})$.

Depth integrated values of WT are gathered in $WT2D$ and for each 2D time step smagor2d.f90 is called to compute $A_{M2Dij} = \max(A_{M2Dij}, WT2D_{ij})$ where A_{M2Dij} first is computed using (18).

We are treating the viscous terms with explicit methods in time. They are subject to the time step limitations

$$\begin{aligned} DT &\leq \frac{\Delta X^2}{16 \max(A_{Mijk})}, \\ DT/N2D &\leq \frac{\Delta X^2}{16 \max(A_{M2Dij})}. \end{aligned}$$

Since A_M and A_{M2D} are determined by the dynamics, it may be difficult to guarantee before the start of a simulation that the above requirements will be fulfilled.

Instabilities will arise when A_M and/or A_{M2D} become large and therefore we have put upper limits on their values according to:

$$A_M \leq \frac{\Delta X^2}{16DT},$$
$$A_{M2D} \leq \frac{N2D \times \Delta X^2}{16DT}.$$

We notice that A_{M2D} may become a factor $N2D$ larger than A_M . Thus, when running a time splitted model the effective horizontal viscosity may be much larger than when running an implicit method with Courant numbers larger than 1 and the same time step for all terms in the equations.

4 The North Sea experiment

The model is implemented for an extended North Sea and horizontally the model domain is discretized in a 20×20 km grid, see Figure 1. Vertically a formulation due to Lynch *et al.* [16] is applied to distribute the σ layers. Let Δ_b be the thickness of the bottom or surface σ layer. Let kb be the number of σ layer interfaces. Define $\Delta_\sigma = \frac{1}{kb-1}$ and $a = (\Delta_\sigma - \Delta_b)/\sin(2\pi\Delta_\sigma)$. The kb layer interfaces may then be defined according to

$$z_k = -1. + (kb - k)/(kb - 1) - a\sin((2\pi(kb - k))/(kb - 1)), k = 1, \dots, kb$$

This choice of layer interfaces gives a smooth distribution of σ layers with thinner layers towards bottom and surface with a proper choice of Δ_b . For $kb = 21$ and $\Delta_b = 0.01$ the thicknesses of the top 10 layers are 0.010, 0.014, 0.021, 0.032, 0.044, 0.056, 0.068, 0.079, 0.086, 0.090 and the distribution is symmetric around the midpoint. The sensitivity of model outputs to the choice of kb will be studied.

The model is run for 30 days from 15/10-89. The model is forced with 6-hourly hindcast atmospheric pressure fields and 6-hourly wind stress fields provided by DNMI [11]. Climatological fields for horizontal velocities, temperature, salinity and surface elevation for October and November are taken from Engedahl *et al.* [13]. Monthly climatological values for these fields are also used as boundary conditions at the open lateral boundaries where we apply a flow relaxation zone that is 7 grid cells wide. See Martinsen and Engedahl [17]. Four components of the tide, M_2 , S_2 , O_1 and K_1 , are forced through the flow relaxation zone using tidal fields provided by the Norwegian Meteorological Institute. The inflow from the Baltic is implemented after an algorithm due to Stigebrandt [24].

The model is run with monthly mean river runoff from the Rhine, Meuse, Scheldt, Ems, Weser, Elbe, Thames, Humber, Tyne and Tees. Daily river runoff from the 6 largest Swedish rivers between Øresund and the Norwegian border is used. The fresh water runoff from the coast of Norway is based on monthly mean fluxes and distributed along the Norwegian coast.

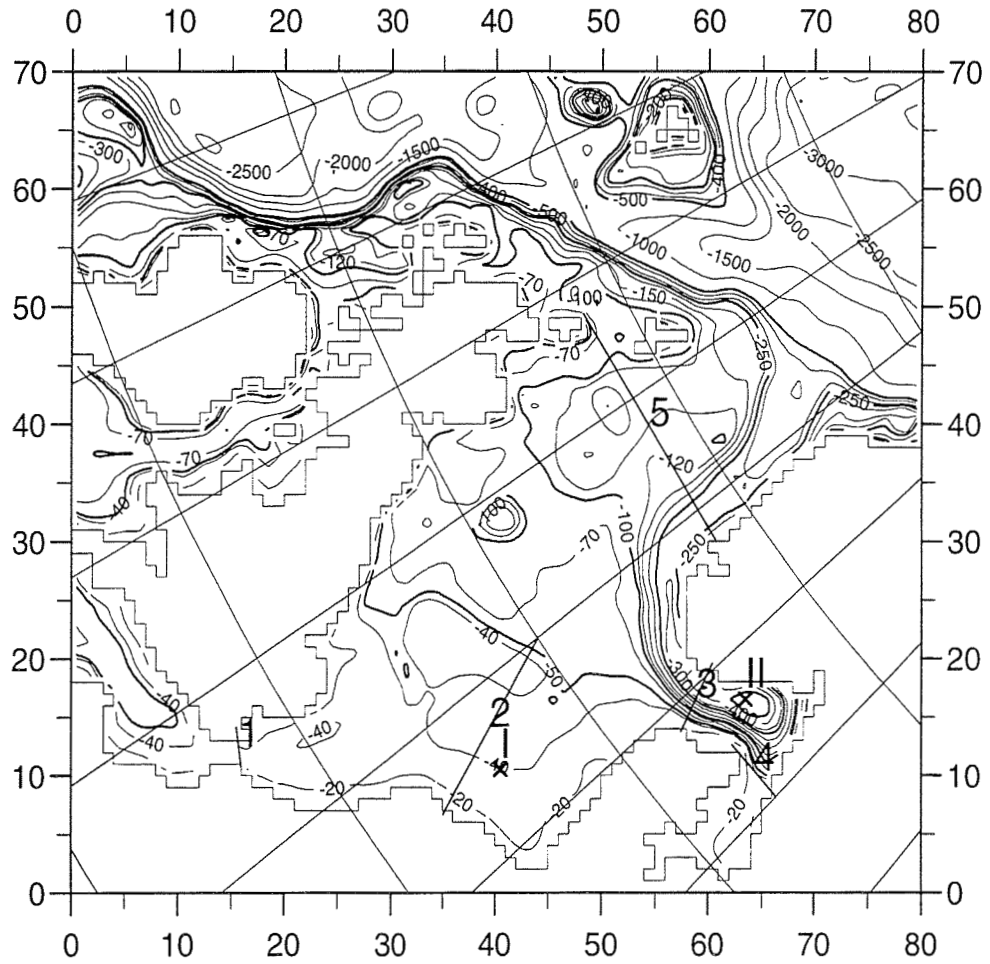


Figure 1. Bottom topography of the North Sea model area. The transects are numbered from 1 to 5. The stations are numbered I and II.

5 Data from the Utsira-Orkneys transect

Across the transect from Utsira to the Orkneys 18960 observations of salinity and temperature were made in the months October and November in the period from 1972 to 1996 by research vessels from the Institute of Marine Research, Norway. The observations are from 31 different surveys in this period. Time averages of salinity across the transect for October-November computed from this dataset are shown in Figure 2. The corresponding standard deviations in the salinity field reflecting the temporal variability are given in Figure 3.

From Figure 2 we notice at the west side of the Norwegian trench the inflow of core Atlantic water. At the east side the outflow of the Norwegian Coastal Current (NCC) is apparent. The offshore deepening and the onshore lifting of the salinity contours are remarkable features. A permanent (at least for this period of the year) cyclone may explain this deepening-lifting effect. We also notice that the core of the NCC in average is found off-shore. The standard deviation contours are also related to the NCC with a maximum towards the surface close to the Norwegian coast. A maximum is also found close to the Orkneys.

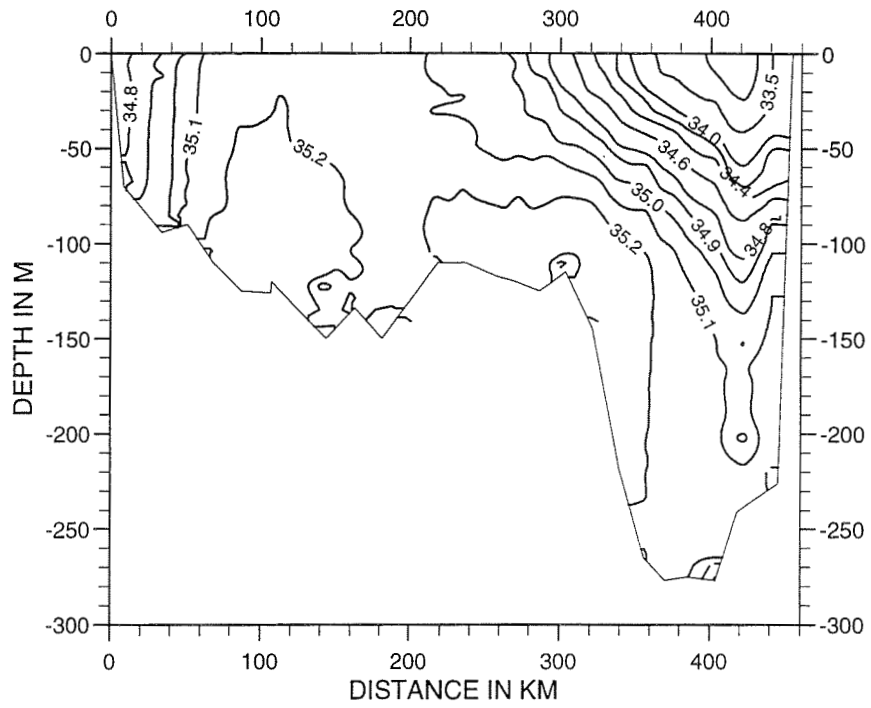


Figure 2. Average salinity in p.s.u. for October and November for the years 1972 to 1996 for the Utsira-Orkneys transect (transect 5).

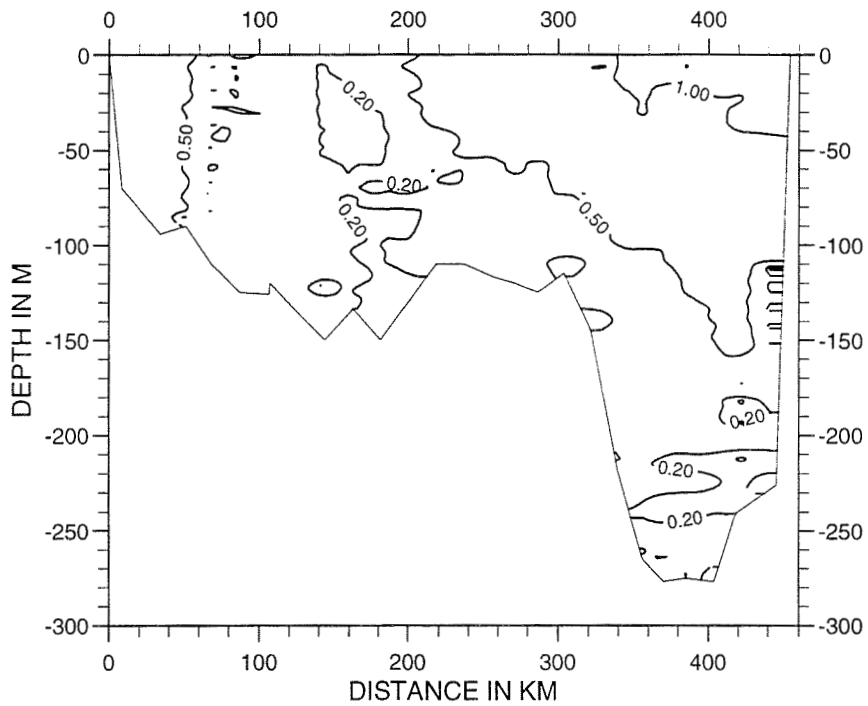


Figure 3. Standard deviations of the salinity fields for the Utsira-Orkneys transect (also in p.s.u.).

6 Results from the climatology

In many major applications of ocean models it is more important to have the major transports correct than to capture detailed features correctly in space and time. The transports based on time averaged velocities through the following transects, see Figure 1, are therefore computed

Transect number	From	To	Name	Direction
1	(50 ⁵⁵ , 1 ⁵⁵)	(51 ¹⁰ , 1 ⁰⁵)	English Channel	Eastward
2	(53 ¹⁰ , 6 ⁰⁰)	(56 ⁰⁰ , 4 ⁰⁰)	Southern North Sea	Eastward
3	(57 ⁰⁰ , 8 ⁴⁰)	(58 ⁰⁴ , 7 ⁵⁰)	Skagerrak	Westward
4	(57 ³⁰ , 10 ⁰⁰)	(57 ³⁰ , 12 ⁰⁰)	Kattegat	Northward
5	(59 ²⁸ , -3 ⁰⁰)	(59 ²⁸ , 5 ¹¹)	Orkneys-Utsira	Northward

Table 1. Table of transects through which residual transports are estimated.

Climatologies [13] are used as initial and boundary values in the numerical experiments to be described, and it is interesting to compare these fields both to the measurements across the Utsira-Orkneys transect and to the model outputs from the present model. The climatologies are produced with a version of the Blumberg and Mellor model [7] using 20km horizontal resolution, see [13]. In Table 2 volume fluxes produced from the velocities in the climatologies are given.

Transect number	Transports October	Transports November
1	92640.	58780.
2	520600.	622800.
3	1690000.	1838000.
4	32210.	35390.
5	2512000.	2442000.
3-35	182600.	161000.
4-33	0.	0.

Table 2. Table of volume fluxes based on monthly mean velocities for October and November from the climatology [13] in m^3s^{-1} through transects 1 to 5 above the horizontal separation line. Below the separation line the fluxes computed from the climatology of water with salinity greater or equal to 35.0 p.s.u. into Skagerrak through transect 3 and the fluxes of water with salinity greater or equal to 33.0 p.s.u. into Kattegat in m^3s^{-1} are given for the two months.

The salinities from the climatologies for the months October and November across

the Utsira-Orkneys transect are given in figures 4 and 5. Comparing these figures with the time average from measurements, Figure 2, we find:

- The core of inflowing Atlantic water with salinity greater than 35.2 p.s.u. is reproduced, but it is located on the shelf instead of at the shelf edge.
- The minimum value in value in salinity of the outflowing NCC water is well reproduced. That is, we find cores of water with salinity less than 33.0 p.s.u. both in the climatologies and in Figure 2. However, the minimum values are found on-shore in the climatologies and off-shore in Figure 2.
- The remarkable onshore lifting of the salinity contours in Figure 2 is not reproduced in the climatologies.
- The water masses in the deeper parts of the Norwegian trench are excessively mixed in the climatology. For instance the 35.0 p.s.u. contours extends to the bottom ($\sim 270\text{m}$) both in Figure 4 and in Figure 5 whereas the maximum depth of this contour in Figure 2 is approximately 130m. The horizontal gradients in salinity, and thus in density, in the deeper parts of the Norwegian trench are thus much larger in the climatologies than in the time average from measurements. Applying the salinities from the climatologies as a driving force in model studies may therefore give unrealistically large currents.

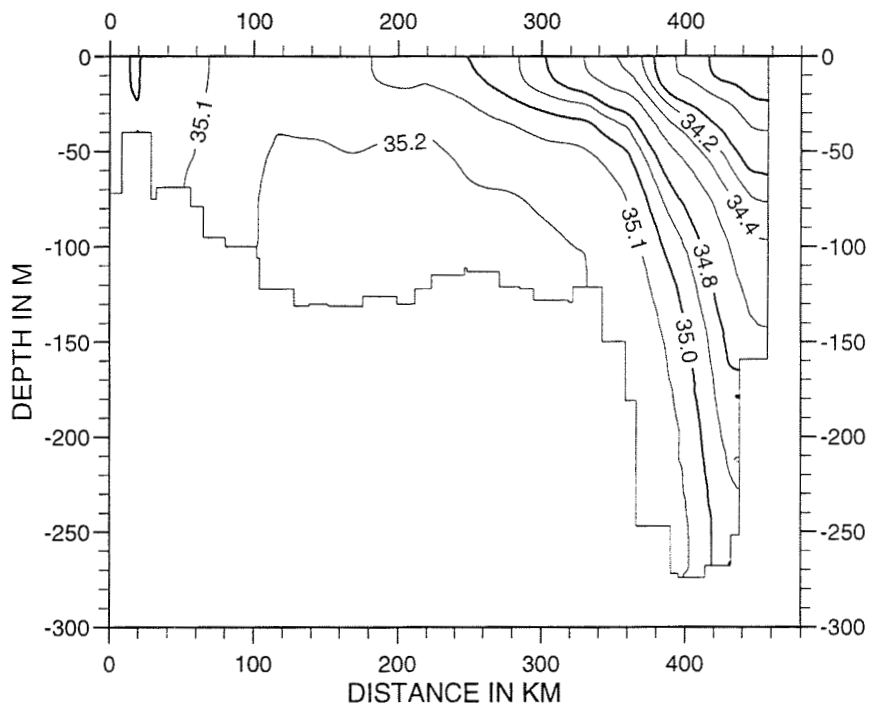


Figure 4. Salinity in p.s.u. from the climatology for October for the Utsira-Orkneys transect.

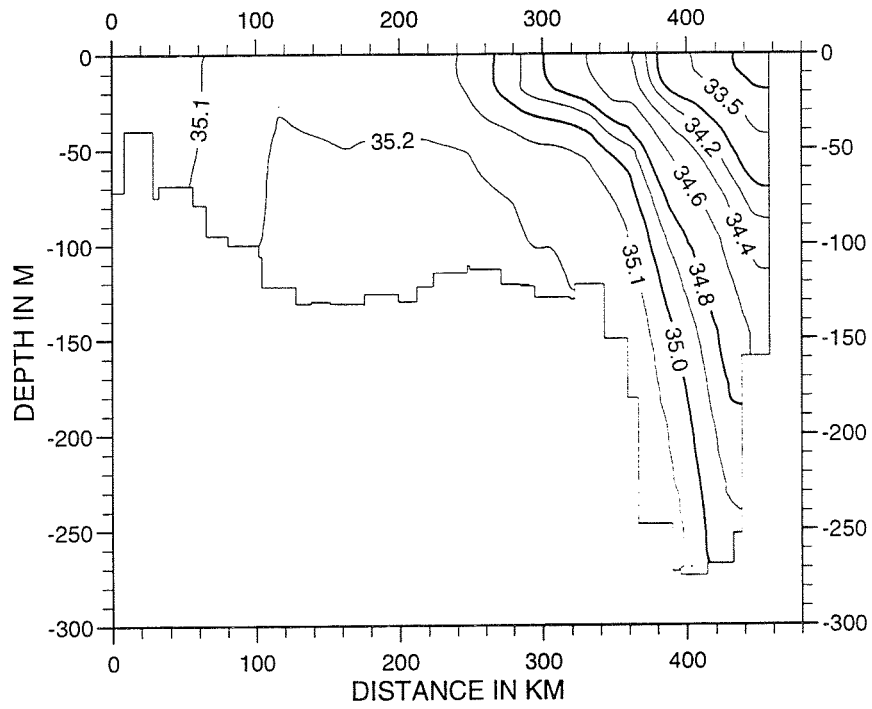


Figure 5. Salinity in p.s.u. from the climatology for November for the Utsira-Orkneys transect.

7 Sensitivity to the vertical resolution

To quantify how many vertical layers that are needed in numerical simulations of flow in stratified oceans is very difficult. It is also unclear how a fixed number of layers should be distributed. The answers will depend on the specifics, topography, tidal effects, river runoffs etc., for the region of the ocean that we focus on. The answers will to a great extent depend on the models abilities to preserve fronts horizontally and vertically. That is: both the choice of turbulence models, with minimum allowed values of diffusivities and viscosities, and advection schemes become important. The answers will also depend on the applications in mind. Is it important to get vertical profiles of the velocities correct, or are we satisfied with realistic values of residual transports.

In a recent study Lynch *et al.* [16] focus on grid convergence on Georges Bank. They conclude that proper resolution of vertical processes is possible with 20 to 30 smoothly graded vertical layers. Their study is for a non-stratified ocean. Davies and Xing [9] demonstrate that stratification will have a significant effect on vertical profiles of velocities, diffusivities and viscosities, and discuss the need for validation of turbulence closure models for stratified cases.

In this section results from the numerical experiments, with methods and parameters as described in section 3. are given. The model area and forcing is described in section 4. The internal time step, DT , is chosen to be 300s and the external time step $DT/N2D$, is chosen to be 50s. The sensitivity of the results to the vertical resolution will be in focus and the model is run with 6, 11, 21 and 31 vertical σ -interfaces. In Figure 6 the salinities across the Utsira-Orkneys transect after 30 days (14/11-89) run with the model are given.

Comparing Figure 6 with Figure 2, having the standard deviations (Figure 3) in mind, we find that the model salinities across this transect are less than one standard deviation off the average for this period of the year. The model contours, however, are in places too steep indicating excessive vertical exchange processes in the model. The minimum value of the model salinity is approximately 33.0, which is in good agreement with the minimum value in the time average from observations. The location is, however, on-shore instead of off-shore like in the climatologies. The remarkable 'dip' in the salinity contours in Figure 2 is not reproduced by the model even if we can see small indications in some contours in Figure 4.

Comparisons of the outputs from the climatologies given in figures 4 and 5 with Figure 6 must be done with caution because the fields in Figure 6 represent 25 hour averages for a specific year. However, we have observed similar struc-

tures for other years with different wind fields, indicating that it is the baroclinic forcing that sets up the main density/salinity structure and that variations in the atmospheric forcing gives perturbations on this. The lateral extent of the NCC in the surface water of the climatology seems to be in better agreement with measurements than the fields in Figure 6. On the other hand the excessive down mixing in the Norwegian trench is at least reduced even if the 34.8 to 35.1 contours still go to deep towards the Norwegian coast. This means that we may have a more realistic baroclinic forcing in the deeper parts of the Norwegian trench.

We find only a small improvement when the vertical resolution is improved. Following the 35.0 and 35.1 contours we note some improvements when we go from Figure 4a to 4d, but we find no changes in the major features. To go from $kb = 21$ to $kb = 31$ gave no noticeable improvement.

In Table 3 monthly means of the residual transports, computed from 25 hourly means of velocities, for different values of kb and Δ_b are given. The maximum layer thicknesses Δ_{max} are also indicated

kb	$\Delta_b(\Delta_{max})$	Transect 1	Transect 2	Transect 3	Transect 4	Transect 5
6	0.05(0.400)	112543.	782439.	234567.	58689.	858582.
11	0.02(0.180)	114113.	780360.	239696.	58346.	859817.
21	0.01(0.090)	113634.	775657.	230413.	57395.	852296.
31	0.01(0.060)	114943.	777221.	229644.	57414.	850946.

Table 3. Table of monthly means of residual volume fluxes in m^3s^{-1} through transects 1 to 5.

In Table 4 the fluxes of water with salinity greater or equal to 35.0 p.s.u. into Skagerrak through transect 3 and the fluxes of water with salinity greater or equal to 33.0 p.s.u. into Kattegat through transect 4 are given.

kb	Transect 3-35	Transect 4-33
6	76803.	3472.
11	79298.	6625.
21	78547.	7439.
31	75763.	7865.

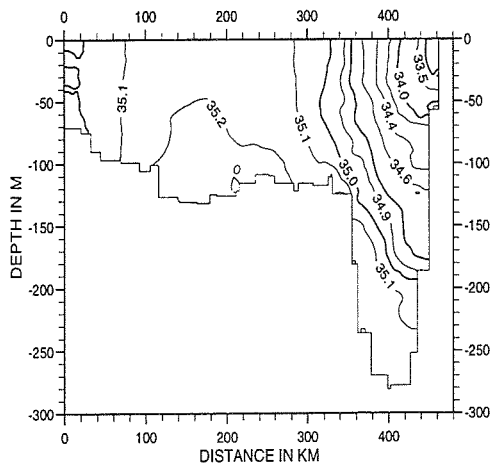
Table 4. Table of fluxes of water with salinity greater or equal to 35.0 p.s.u. into Skagerrak through transect 3 and the fluxes of water with salinity greater or equal

to 33.0 p.s.u. into Kattegat in m^3s^{-1} .

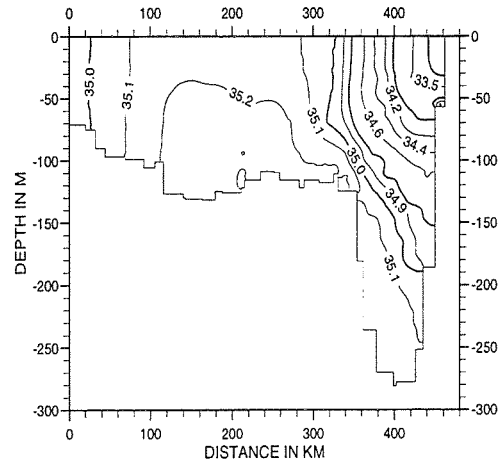
From Table 3 we note that the residual transports are not very sensitive to the number of σ -coordinate layers in the present study. Also the transports of 35.0 p.s.u. water into Skagerrak (Table 4) are not affected much by changes in the vertical resolution. Only for the transports of 33.0 p.s.u. water into Kattegat we notice a clear effect of improving the vertical resolution. This transect, however, is only covered by 4 horizontal grid cells and the processes of this region are far from resolved.

The transports in/out of Skagerrak are estimated to be approximately 1 Sv ($= 1 \times 10^6 m^3 s^{-1}$) and the transports northwards along the Norwegian coast further north somewhat larger. The model transports for transect 5 and especially the Skagerrak transect (transect 3) seem therefore to be too small. The transports computed from the climatologies, Table 2, are also much larger for these transect. That the transports are small is not surprising since we have run the model with very large values of horizontal viscosities to avoid excessive vertical exchange due to large oscillations in the vertical velocities. The depth averaged horizontal viscosities, A_{M2D} , are given in Figure 7. The values are in most of the area higher than $100000 m^2 s^{-1}$, and in the NCC and the Skagerrak the values are almost $500000 m^2 s^{-1}$ which is the maximum allowed value in this experiment. Here the baroclinic forcing creates small scale, compared to the grid size, vertical oscillations and the model responds by enhancing the horizontal viscosities.

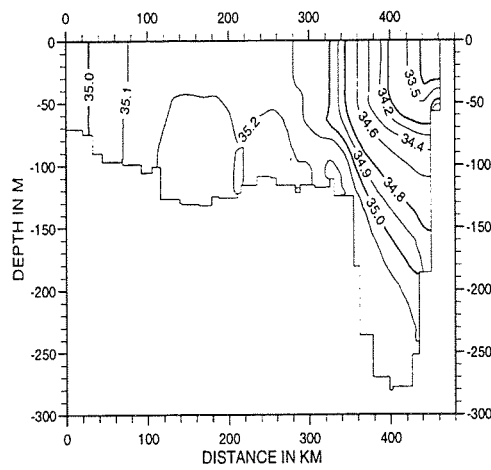
In Figure 8 vertical profiles of the viscosity, KM , and the V-component of the velocity over a tidal cycle are given for $kb = 6, 21$ and 31 at station I, Figure 1. Here the water masses are non-stratified and the vertical profiles smooth. There are small differences when we enhance the resolution from 21 to 31 layers. In Figure 9 the corresponding profiles for station II, Figure 1, are given. Station II is located in the Skagerrak where the water is stratified and we notice the effects of this both on the viscosities and on the velocities. In the deeper parts of the Skagerrak the viscosities are much smaller than in the open North Sea due to the stratification. Refining the grid resolution from 21 to 31 layer has clear effects on the profiles of KM , but only minor effects on the profiles of the velocities. In Figure 10 the model salinities at 10m depth for $kb = 21$ at the end of the simulation are given.



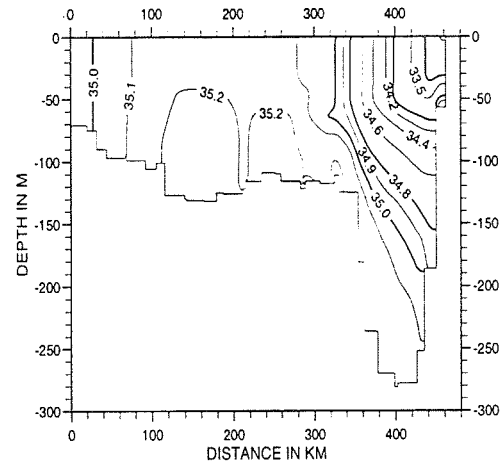
(a) $kb=6$



(b) $kb=11$



(c) $kb=21$



(d) $kb=31$

Figure 6. Model salinity in p.s.u. for 14/11-89 for the Orkneys to Utsira transect. 25 hour averages are given.

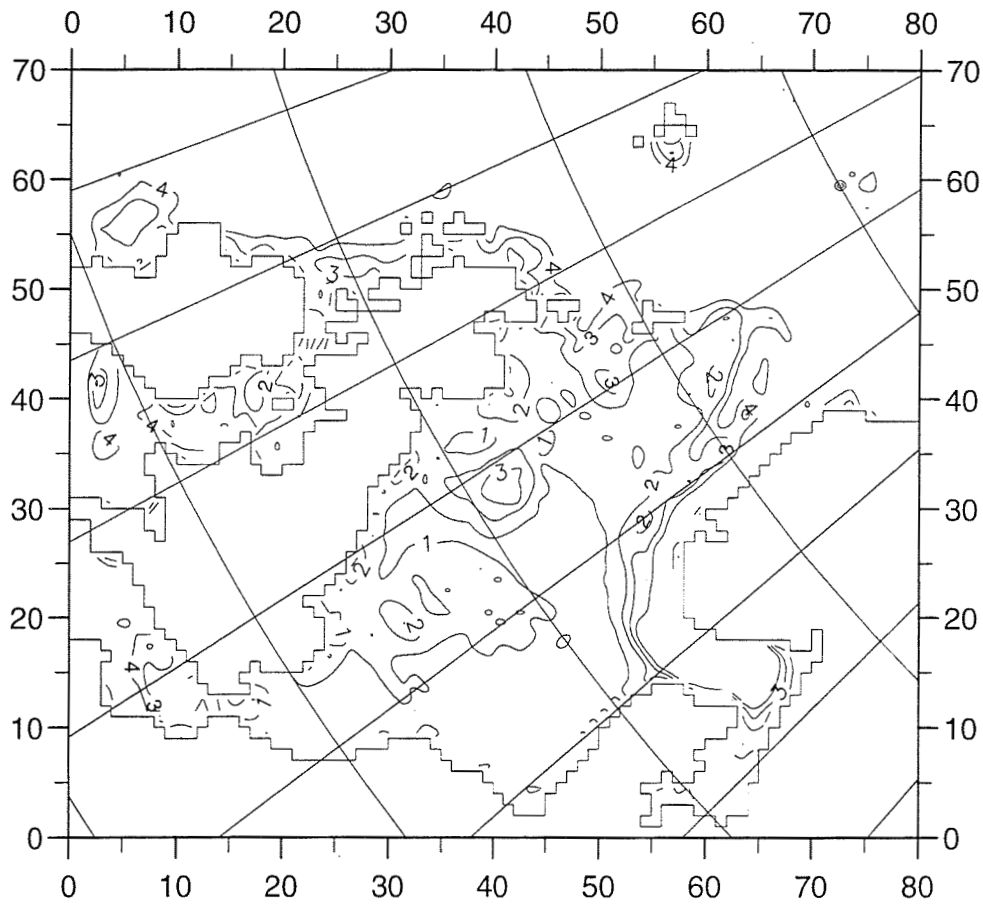


Figure 7. Values of A_{M2D} in $100000m^2s^{-1}$ for $kb = 21$. The values are averaged in time over the period from 15/10-89 to 14/10-89.

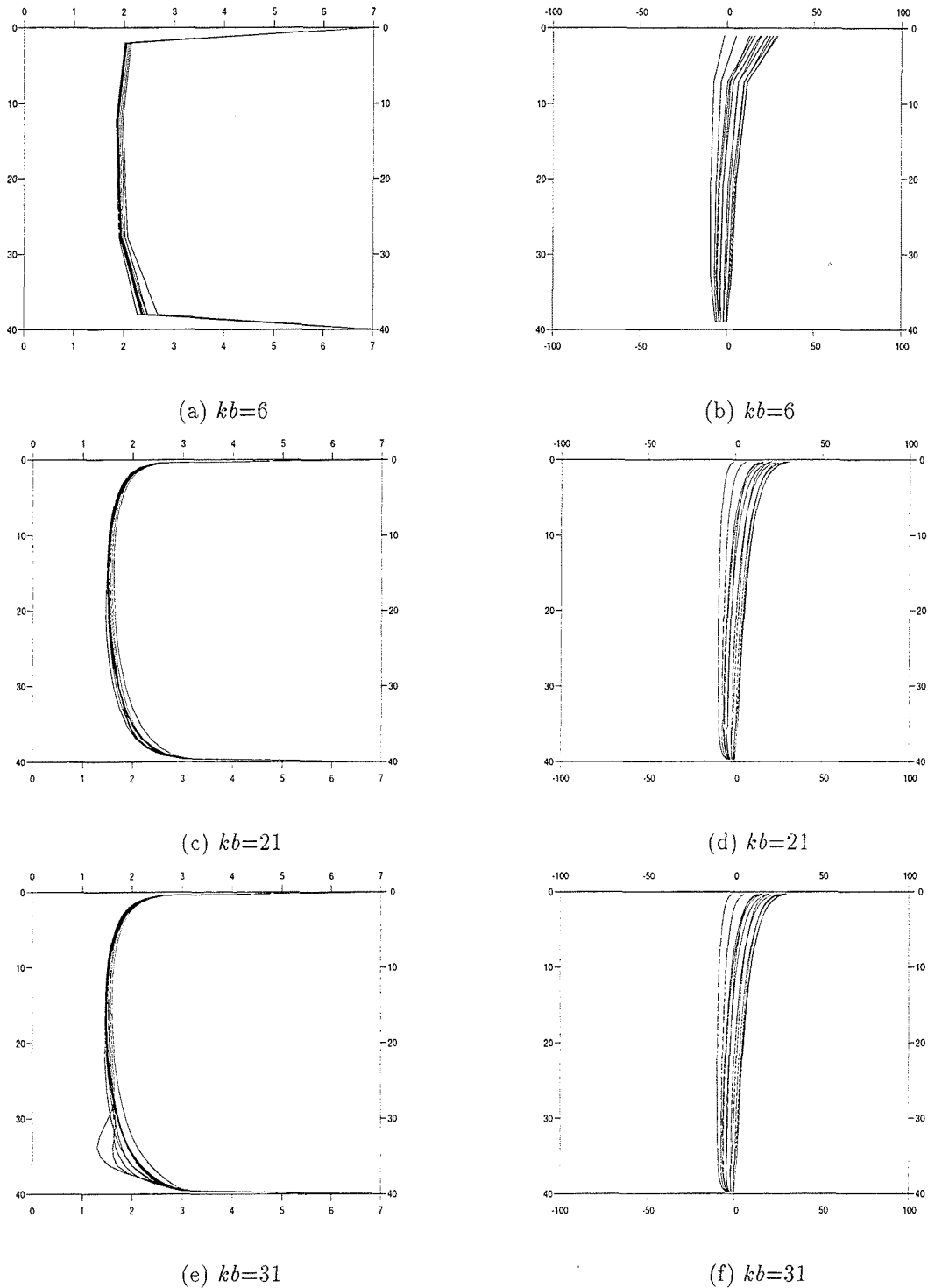


Figure 8. Vertical profiles of the viscosity(KM) (left panel) and the V-component of the velocity (right panel) at grid cell (41,11), station I in Figure 1. The unit on the vertical axis is depth in m . For the diffusivities the unit on the horizontal axis is $-\log_{10}(KM)$. For the velocities the unit is $cm\ s^{-1}$. In the top panel results for $kb = 6$ are given, in the middle panel $kb = 21$ and in the bottom panel $kb = 31$. The profiles are taken 300, 301, ..., 312 hours after the start of the simulation.

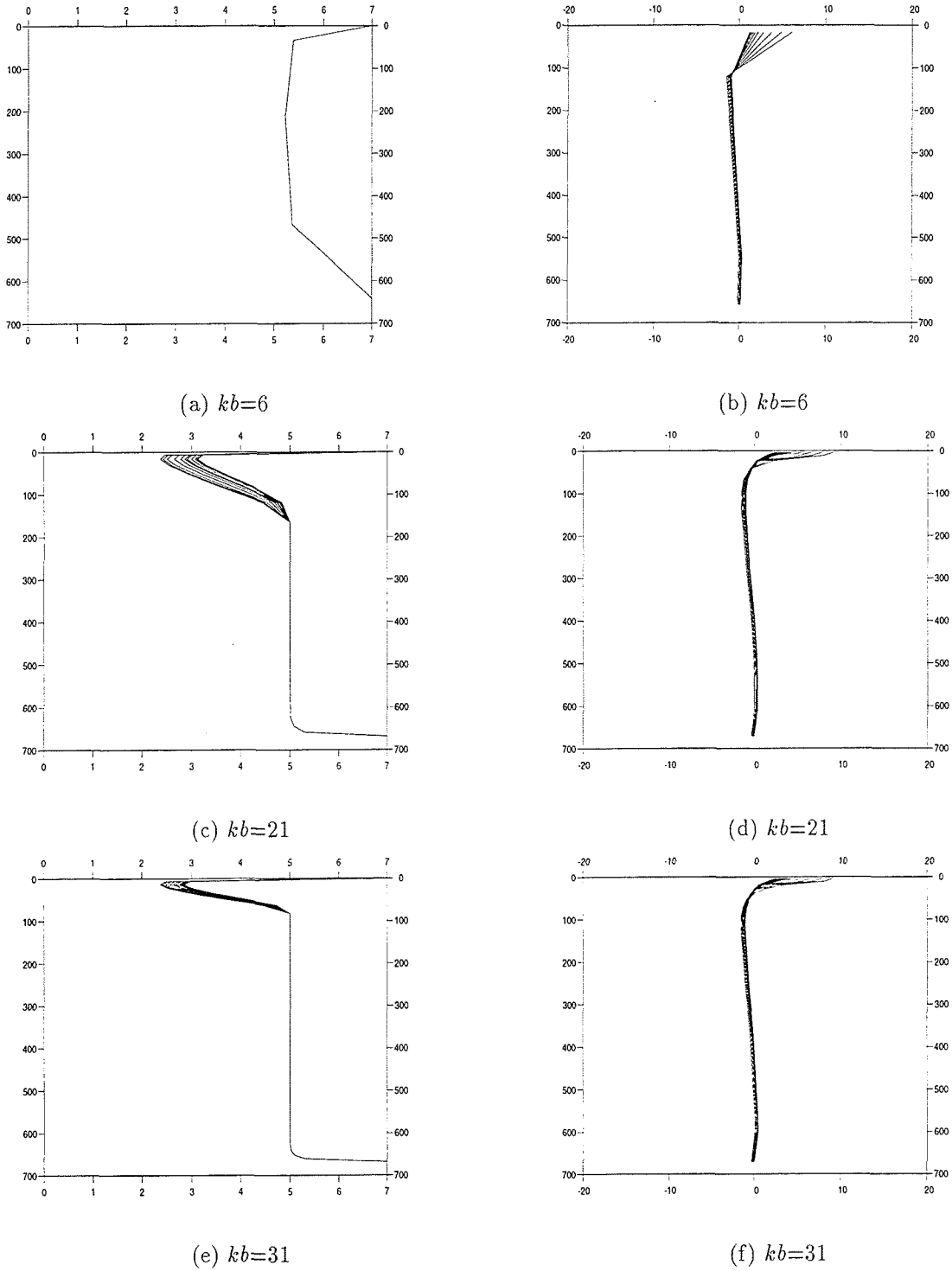


Figure 9. Vertical profiles of the viscosity (left panel) and the U -component of the velocity (right panel) at grid cell (64,17), station II in Figure 1. The unit on the vertical axis is depth in m . For the viscosities the unit on the horizontal axis is $-\log_{10}(KM)$. For the velocities the unit is $cm s^{-1}$. In the top panel results for $kb = 6$ are given, in the middle panel $kb = 21$ and in the bottom panel $kb = 31$. The profiles are taken 300, 301, ..., 312 hours after the start of the simulation.

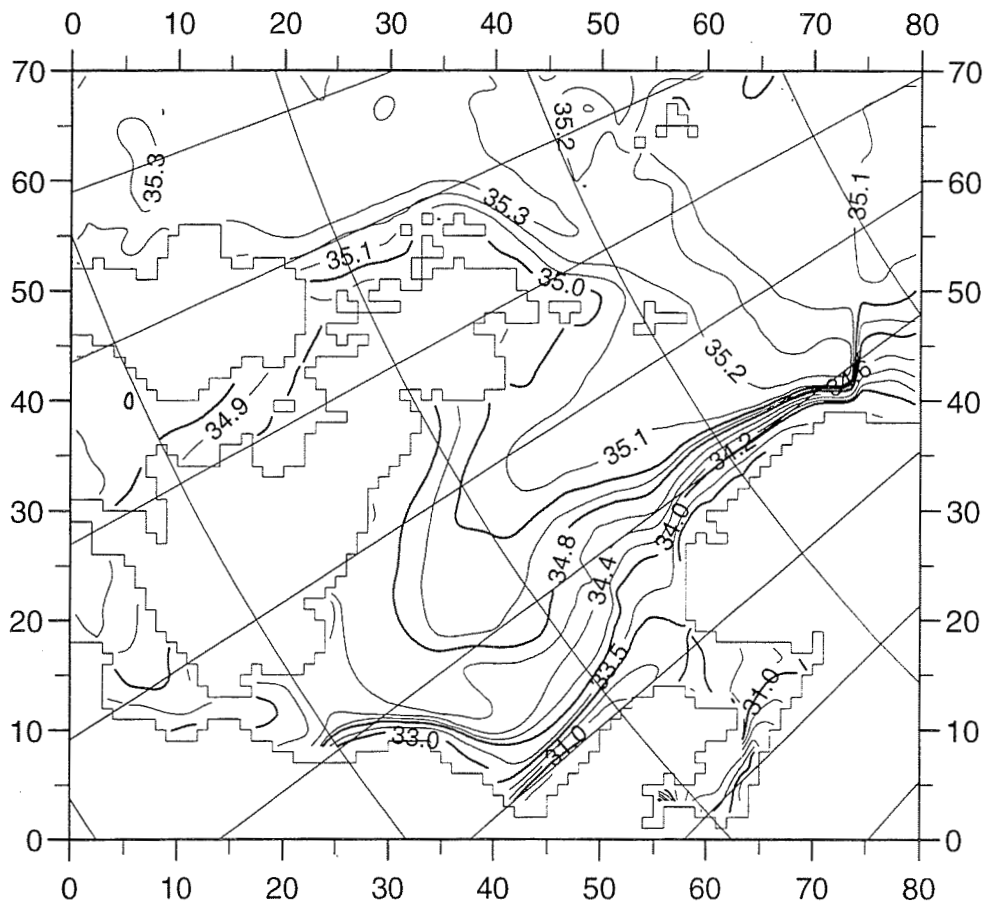


Figure 10. Model salinities in p.s.u. at 10m depth for $kb = 21$ at the end of the simulation.

8 Sensitivity to the horizontal viscosity - A_M

In the experiments described in the previous section the algorithm from section 3.2.1 was applied to enhance the horizontal viscosities, A_M . In the present section we describe some very noticeable effects of this enhancement by giving results from an experiment with $C_{M2} = 0.0$ and $C_M = 1.0$ (as before) in the Smagorinsky formulation (18). The time steps are as before $DT = 300s$ and $DT/N2D = 50s$. 21 vertical σ -interfaces are used. In Table 5 the transports are given. In Figure 11 the salinities across the Utsira-Orkneys transect after 30 days run with the model are given. In Figure 12 the depth averaged horizontal viscosities, A_{M2D} , are given. In Figure 13 the model salinities at 10m depth at the end of the simulation are given.

Comparing Table 5 and the figures from the present section with the corresponding figures in the previous sections we find:

- All transports are very sensitive to the choice of algorithm and parameters for A_M in a North-Sea experiment with the present horizontal resolution. The transports become as expected much larger as A_M is reduced.
- For the English Channel transect and the Southern North Sea transect the present transports are also larger than the transports in the climatologies.
- For the Skagerrak transect the transports in the climatologies are still larger than the present transports.
- For the Utsira-Orkneys transect the present transports are somewhat larger than the transports from the climatologies. From Figure 11 we note that this large transport may be due to unrealistically large internal pressure gradients which again are due to excessive vertical oscillations. The problem with large pressure gradients in the deeper parts of the Norwegian trench causing possibly unrealistically large transports discussed in the climatology section is therefore even worse with the present model and the present choice of algorithm for A_M (and A_H which so far has been set to zero).
- Comparing figures 12 and 7 we find that the viscosities are typically 2 orders of magnitude smaller in the present run than with the algorithm given in section 3.2.1
- Comparing the horizontal salinity fields in figures 10 and 13 we find that the gradients are much stronger in the present study. This is caused mainly by the reduced viscosities, but we must also bear in mind that A_H is set to zero and that we are using a gradient preserving TVD-scheme for advection.

Transect number	Transports
1	273020.
2	1135057.
3	1190450.
4	92089.
5	2653714.
3-35	114084.
4-33	8293.

Table 5. Table of monthly means of residual volume fluxes in m^3s^{-1} through transects 1 to 5 in m^3s^{-1} through transects 1 to 5 above the horizontal separation line. Below the separation line the fluxes computed from the climatology of water with salinity greater or equal to 35.0 p.s.u. into Skagerrak through transect 3 and the fluxes of water with salinity greater or equal to 33.0 p.s.u. into Kattegat in m^3s^{-1} are given for the two months.

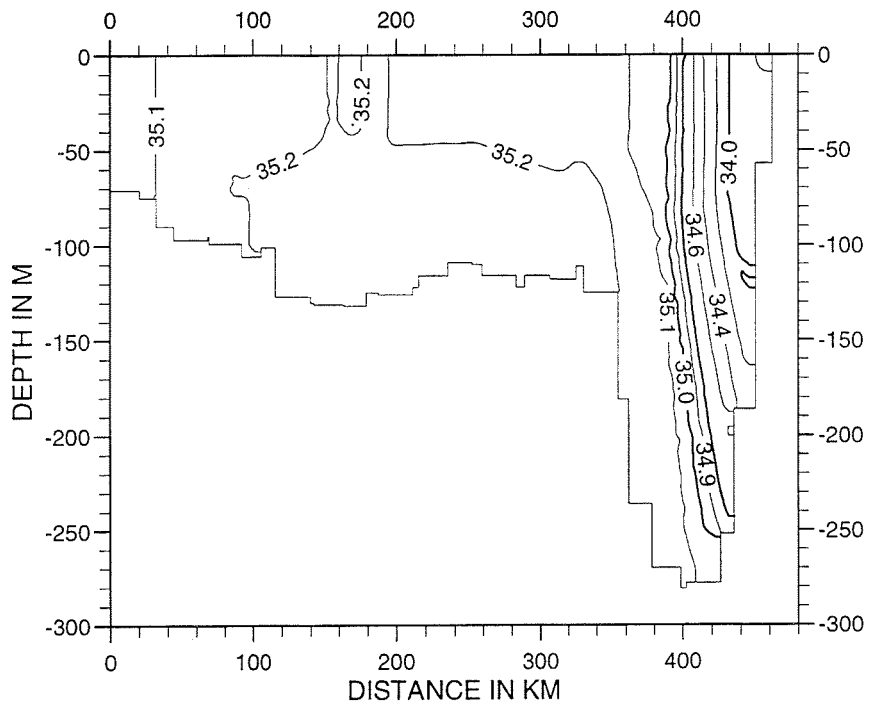


Figure 11. Model salinity in p.s.u. for 14/11-89 for the Utsira-Orkneys transect. 25 hour averages are given.

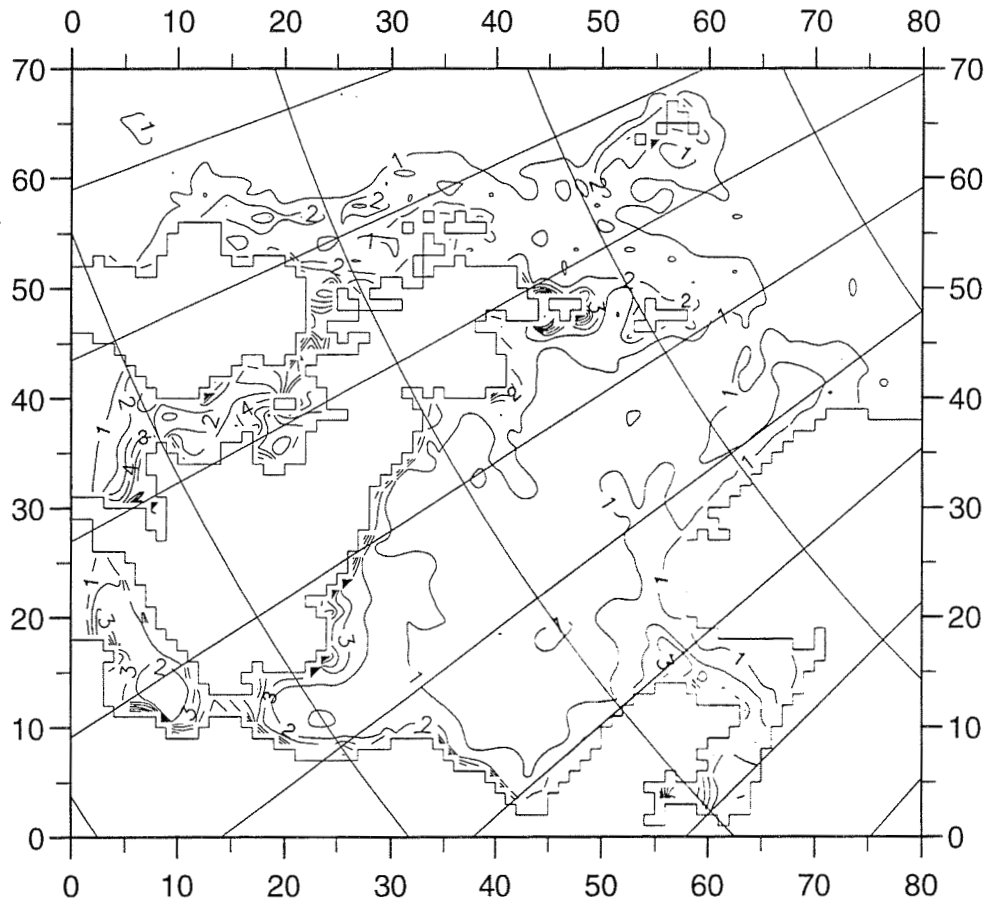


Figure 12. Values of A_{M2D} in $1000m^2s^{-1}$. The values are averaged in time over the period from 15/10-89 to 14/10-89.

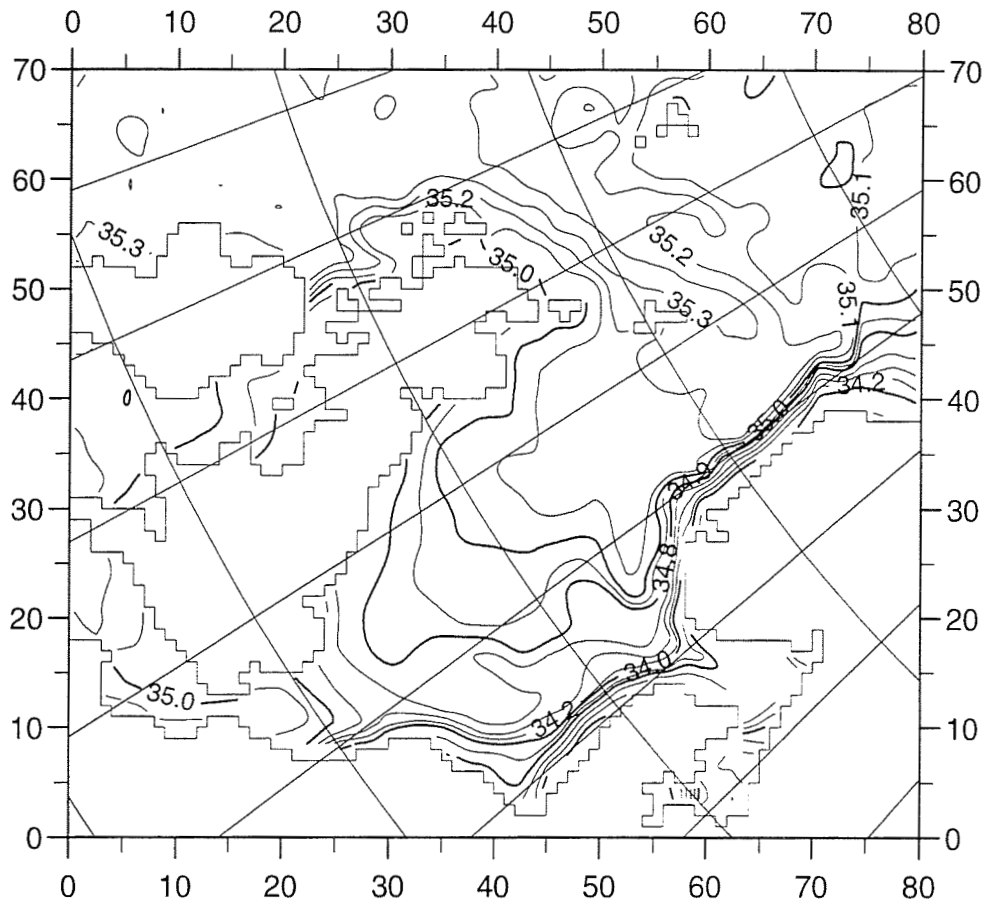


Figure 13. Model salinities in p.s.u. at 10m depth at the end of the simulation.

9 Effects of including horizontal diffusivity - A_H

In our numerical studies so far the diffusivities, A_H , has been set to zero. In the previous section it was shown that this choice in combination with reduced values of A_M gave unrealistically strong internal pressure gradients between the inflowing and outflowing water masses along the Norwegian trench. In the present section the effects of including horizontal diffusion is therefore studied. We have chosen to set $A_H = A_M$ and apply the Smagorinsky formulation (18) with $C_M = 1.0$ (as before) to compute A_M . Otherwise the model setup is exactly as in the previous section. In Table 6 the transports are given. In Figure 14 the salinities across the Utsira-Orkneys transects after 30 days run with the model are given. In Figure 15 the depth averaged horizontal viscosities, A_{M2D} , are given. In Figure 16 the model salinities at 10m depth at the end of the simulation are given.

Comparing tables 5 and 6 we find that the transports through the Southern North Sea transect (number 2) have been very little affected. This could be expected since this transect is located in an area with little baroclinic forcing. The transports through the Skagerrak transect (number 3) and the Utsira-Orkneys transect (number 5) are reduced. This may be explained by a much smoother density field and smaller internal pressure gradients due to the introduced diffusivity. We also note that the introduction of diffusivity with the present algorithm reduced the transport of Atlantic water with salinity greater than 35.0 p.s.u into the Skagerrak to almost zero. The effect of the horizontal diffusivity on the salinity field is also very noticeable when we compare figures 11 and 14 for the vertical and figures 13 and 16 for the horizontal. Comparing figures 12 and 15 we find that at least along the Norwegian trench the values of A_{M2D} tend to be smaller possibly due to a smoother density field and less small scale oscillations in the velocity fields.

Transect number	Transports
1	318513.
2	1159636.
3	997303.
4	107781.
5	2246036.
3-35	91.
4-33	11404.

Table 6. Table of monthly means of residual volume fluxes in m^3s^{-1} through transects 1 to 5 in m^3s^{-1} through transects 1 to 5 above the horizontal separation line. Below the separation line the fluxes computed from the climatology of water

with salinity greater or equal to 35.0 p.s.u. into Skagerrak through transect 3 and the fluxes of water with salinity greater or equal to 33.0 p.s.u. into Kattegat in m^3s^{-1} are given for the two months.

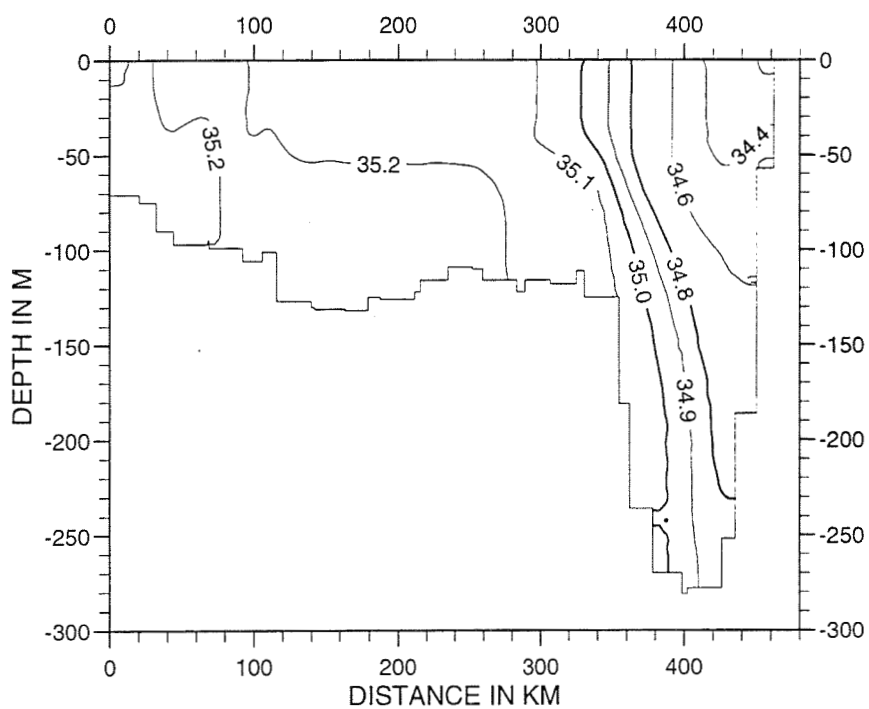


Figure 14. Model salinity in p.s.u. for 14/11-89 for the Orkneys to Utsira transect. 25 hour averages are given.

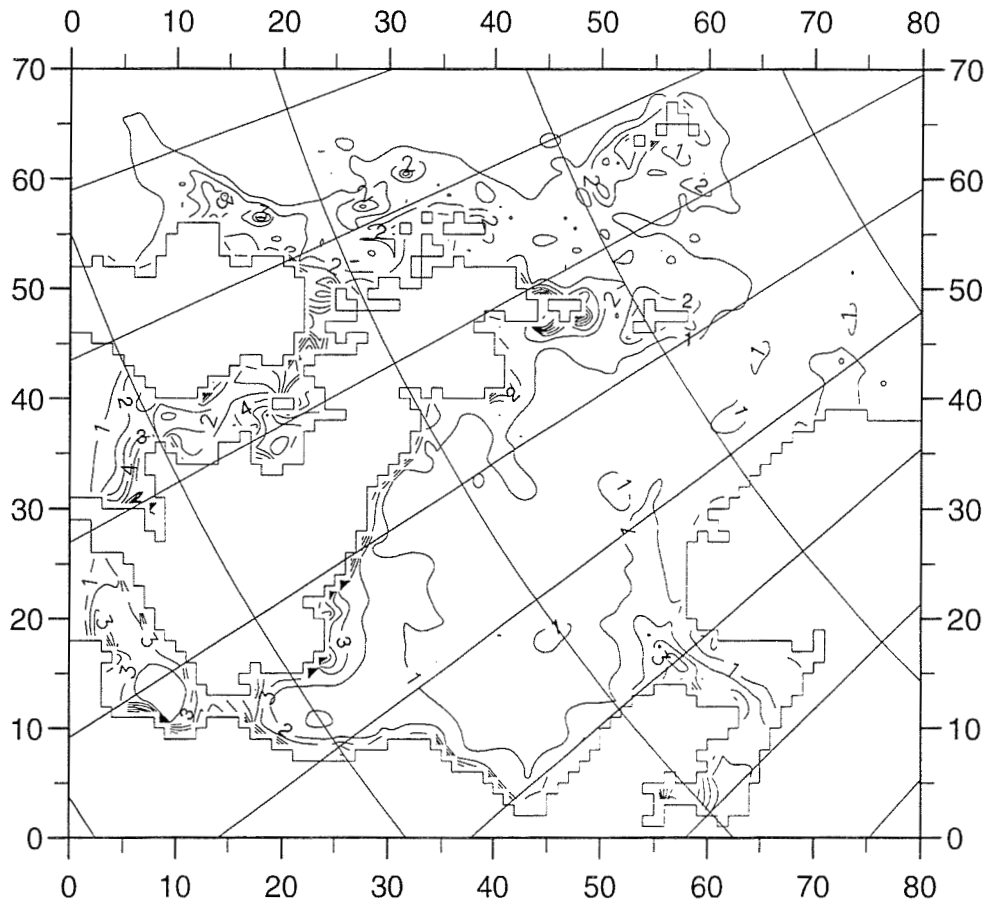


Figure 15. Values of A_{M2D} in $1000m^2s^{-1}$. The values are averaged in time over the period from 15/10-89 to 14/10-89.

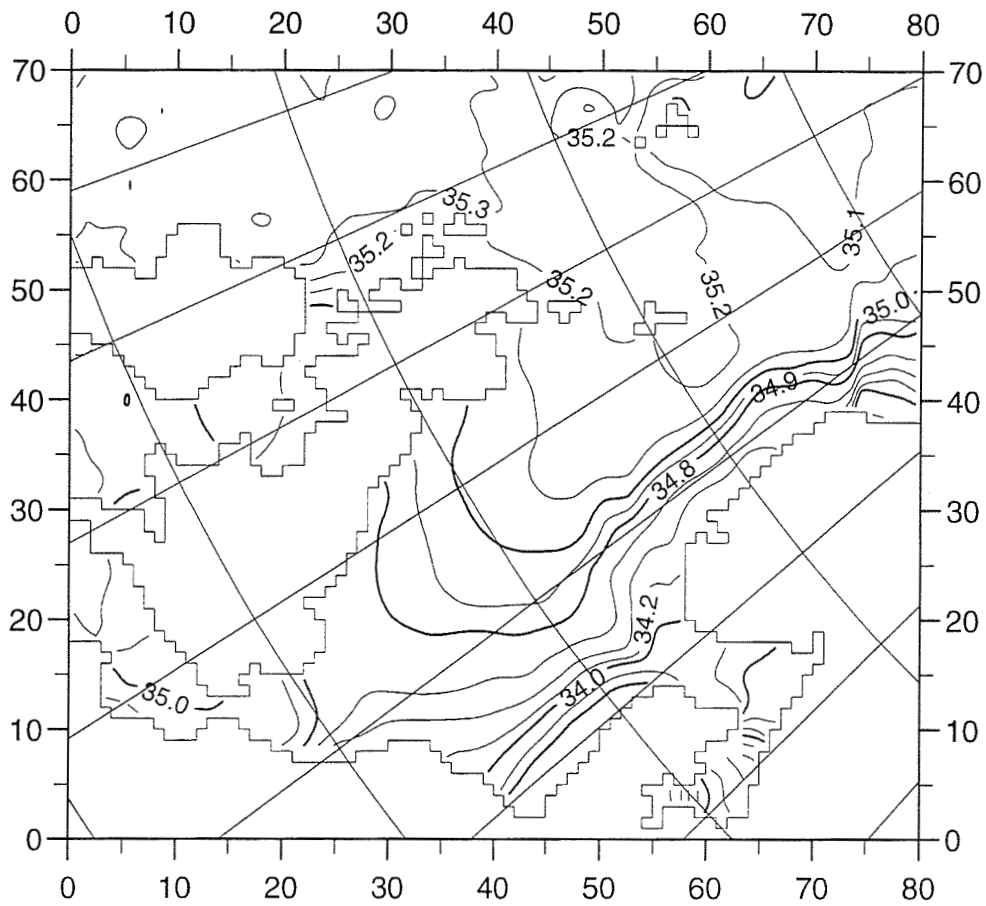


Figure 16. Model salinities in p.s.u. at 10m depth at the end of the simulation.

10 Convergence in time

In the present section the convergence properties of the model with respect to the time steps is studied. The responses on the residual transports of various choices of 3-D time steps, DT, and 2-D time steps, DTE, are summarized in tables 7 and 8 below. In Figure 17 the model salinity across the Utsira-Orkneys transect for the experiment with DT = 3600s is given.

We find that with the present time split version of the model the results are robust to the choice of time step. To reduce the 2-D time step from 50s to 25s had only marginal effects on the residual transports and the density field. We have increased the 3-D time step from 150s to 3600s, and even for the longest time steps the errors in for instance the residual transports due to time discretization errors are probably inferior to the errors due to uncertainties in for instance the sub grid scale parametrizations or the horizontal resolution. Comparing figures 14 and 17 we also find only minor differences.

With the present horizontal resolution and sub grid scale parametrizations the results are therefore very robust to the choice of time step as long as the 2-D time step is smaller than the CFL-criterion and the 3-D time step less than 1 hour. With finer horizontal resolution, we will probably benefit from smaller time steps.

DT	DTE	Transect 1	Transect 2	Transect 3	Transect 4	Transect 5
300s	50s	318513.	1159636.	997303.	107781.	2246036.
300s	25s	319392.	1160232.	997560.	107944.	2246393.
150s	25s	318443.	1159432.	995078.	106947.	2239857.
600s	50s	320098.	1161254.	1000700.	109481.	2256178.
900s	50s	321790.	1163064.	1001721.	110622.	2258714.
1800s	50s	331468.	1175282.	1046629.	116216.	2307714.
3600s	50s	336798.	1195589.	1056175.	118894.	2273536.

Table 7. Table of monthly means of residual volume fluxes in m^3s^{-1} through transects 1 to 5.

DT	DTE	Transect3-35	Transect 4-33
300s	50s	91.	11404.
300s	25s	91.	11328.
150s	25s	92.	11472.
600s	50s	91.	11580.
900s	50s	95.	11733.
1800s	50s	89.	12557.
3600s	50s	99.	16890.

Table 8. Table of fluxes of water with salinity greater or equal to 35.0 p.s.u. into Skagerrak through transect 3 and the fluxes of water with salinity greater or equal to 33.0 p.s.u. into Kattegat in m^3s^{-1} .

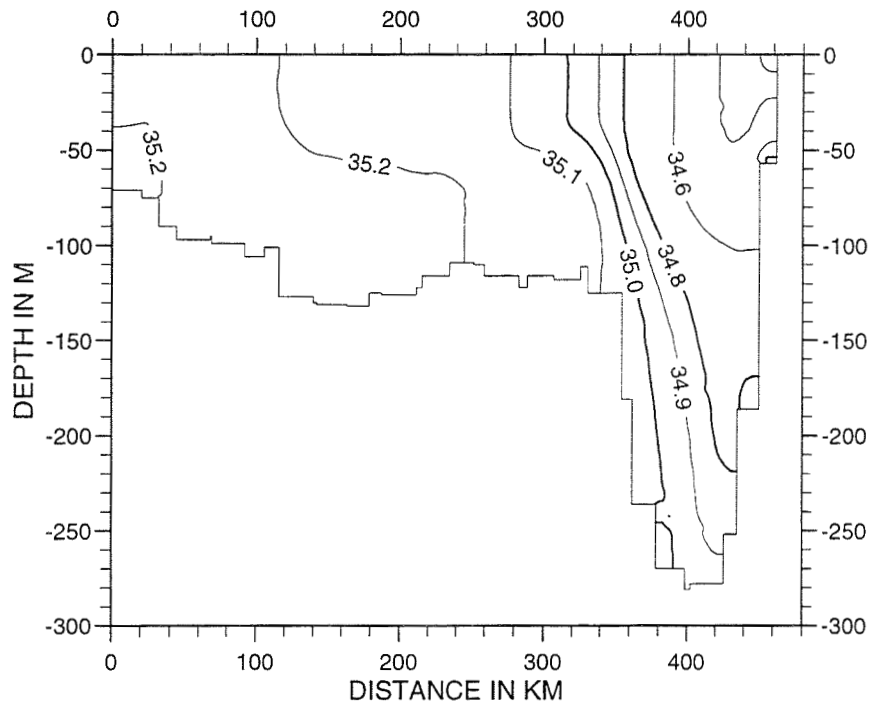


Figure 17. Model salinity in p.s.u. for 14/11-89 for the Orkneys to Utsira transect for $DT = 3600s$. 25 hour averages are given.

11 Discussion

In this paper we have demonstrated that both the residual transports and the models salinity and density structures are very sensitive to the parametrizations of horizontal viscosity and diffusivity in a 20 km resolution baroclinic North Sea model. Smith *et al.* [23] also report on mean transports for various North Sea transects computed with one 2-D barotropic model, POL [14], and two baroclinic 3-D models, IfM [4] and IMR [7, 20]. The horizontal resolution for the two baroclinic models were approximately 20km. Comparing mean transports from the three models over the period 1987-1993, see Table 4 in [23], we find some remarkable differences. The transports through the Northern Skagerrak transect (section 8 in Table 4) is for instance 0.02 Sv (inflowing) for the IfM model and -0.42 (outflowing) for the IMR model. For transects further north across the NCC the results for the IfM model and the IMR model are in better agreement whereas the transports for the barotropic POL model are much smaller.

Along the Norwegian coast we frequently find small scale eddies, $O(10\text{km})$, created by frontal instabilities. These processes are not represented by 20km resolution models. It could be a hope that by choosing good parametrizations for the sub-grid scale processes, the effects on the larger scale fields nevertheless could be well represented. The sensitivity of the transports and the internal pressure field to the horizontal viscosities and diffusivities demonstrated in the present report and the variability documented in [23] are indications on the opposite. The problem with excessive down mixing in the deeper parts of the Norwegian trench reported in the present report, is also apparent from plots of salinity from the prognostic climatology across the Fugløya-Bjørnøya transect (figures 12 and 18 in [13]). The present author has also tried other algorithms and parameter values for parametrizations of sub-grid scale processes in this 20km model, but the numerical evidence points towards the conclusion: By exploiting the degrees of freedom in the parametrizations one may achieve a "fairly good" agreement with observations for one or a few measures. However, other parts of the fields will typically be dubious. With the present model, we could produce a salinity field in fairly good agreement with observations across the Utsira-Orkneys transect at the cost of too small transports. Reasonable transports could also be produced, but then at the cost of unreasonable density gradients across the transect in focus.

In cases where the smaller scale processes are essential for the creation of the larger scale fields, we therefore believe that there is no other solution than to resolve the important smaller scale processes. In [6] the Skagex-dataset [10] was used to validate a 4-km model for the Skagerrak. Even if the horizontal viscosities were only approximately $10\text{m}^2\text{s}^{-1}$ and the diffusivities set to zero, a

better agreement with observed salinity fields was achieved even if the fields still suffers from deficiencies when compared to the solutions set up by nature. Eldevik and Dysthe [12] has studied frontal instabilities similar to those appearing along the Norwegian coast with the version of the present model documented in [5] and 500m horizontal resolution. Both the viscosities and the diffusivities were set to zero, and the effective numerical diffusion near fronts was estimated to be between 10 and 20 m^2s^{-1} . It is shown that with this resolution the spiral eddies are well resolved. The results in Asplin *et al.* [2] produced with 500m resolution also support the hypothesis that with sufficient horizontal resolution the problems with excessive vertical exchange documented in the present report become negligible.

There is thus evidence that with higher resolution these baroclinic instabilities and their effects on the larger scale fields may be better reproduced and that at least 4km resolution is necessary in the Skagerrak and along the Norwegian coast. To run 3-D models for the whole North Sea with high resolution also in the vertical, and a few kilometer horizontal resolution is still very time consuming (if possible at all) on todays computers. The need for models with capabilities for automatic nesting between coarse grid model solutions and finer grid solutions is therefore obvious.

In the case of very large horizontal viscosities it is shown in this report that the results from a 20km model for the North Sea are relatively insensitive to the vertical resolution. There are no clear improvements in the transports or the results for the vertical transect when the number of vertical layers is increased beyond 10. Horizontal viscosity and horizontal resolution is strongly correlated, so with a finer horizontal resolution and smaller horizontal viscosities, we will probably experience clear improvements with higher resolution also in the vertical.

It is shown that with the present time split version of the model the results are robust to the choice of time step. To reduce the 2-D time step from 50s to 25s had only marginal effects on the residual transports and the density field. We have increased the 3-D time step from 150s to 3600s, and even for the longest time steps the errors in for instance the residual transports due to time discretization errors are probably inferior to the errors due to uncertainties in for instance the sub grid scale parametrization or the horizontal resolution. Therefore, as for the vertical resolution, with finer horizontal resolution, we will probably benefit from smaller time steps.

12 Conclusions

a) In this paper we have demonstrated that both the residual transports and the models salinity and density structures are very sensitive to the parametrizations of horizontal viscosity and diffusivity in a 20 km resolution baroclinic North Sea model.

b) The sensitivity is strongly related to smaller scale baroclinic instabilities not resolved by the model. These eddies are of major importance for the creation of also the larger scale density structures along the Norwegian coast. Evidence is given to support the hypothesis that the larger scale fields may not be correctly reproduced by choosing appropriate parametrizations. The major smaller scale processes must be resolved.

c) Many applied oceanographic studies delivering inputs both to science and management are today performed with ocean models with approximately 20km horizontal resolution or they are using as major inputs results from such models. Both the results from Smith *et al.* [23] and the results from the present report are strong indications that we need model results produced with higher horizontal resolution to be able to deliver higher quality inputs to science and management.

d) In a 20 km resolution baroclinic North Sea model it is sufficient with between 10 and 20 σ -layers in the vertical.

e) The present time split σ -coordinate 20 km North Sea model is robust to the choice of time step. 1 hour 3-D steps may be applied without any major degradation of the quality of the output.

References

- [1] B. Ådlandsvik and H. Engedahl. Documentation of a three-dimensional baroclinic sea-model. Technical Report 16/1991/HSM, Institute of Marine Research, Bergen, NORWAY, 1991.
- [2] L. Asplin, A.G.V. Salvanes, and J.B. Kristoffersen. Non-local wind-driven fjord-coast advection and its potential effect on pelagic organisms and fish recruitment, 1998. Accepted by Fisheries Oceanography.
- [3] R. Asselin. Frequency filters for time integration. *Mon. Weather Rev.*, 100:487-490, 1972.
- [4] J.O. Backhaus and D. Hainbucker. A finite difference circulation model for shelf seas and its application to low frequency variability on the North European Shelf. In J.C.L. Nihoul and B. Jamart, editors, *Three-Dimensional Models of Marine and Estuarine Dynamics*, pages 221-244. Elsevier, Oceanography Series 45, 1987.
- [5] J. Berntsen, M.D. Skogen, and T.O. Espelid. Description of a σ -coordinate ocean model. Technical Report Fisker og Havet Nr. 12, Institute of Marine Research, 1996.
- [6] J. Berntsen and E. Svendsen. Using the Skagex dataset for evaluation of ocean model skills, 1998. Accepted by Journal of Marine Systems.
- [7] A.F. Blumberg and G.L. Mellor. A description of a three-dimensional coastal ocean circulation model. In N. Heaps, editor, *Three-Dimensional Coastal Ocean Models, Vol.4*. American Geophysical Union, 1987.
- [8] M.D. Cox. A mathematical model of the Indian Ocean. *Deep-Sea Res.*, 17:47-75, 1970.
- [9] A.M. Davies and J. Xing. An intercomparison and validation of a range of turbulence closure schemes used in three dimensional tidal models. In D.R. Lynch and A.M. Davies, editors, *Quantitative Skill Assessment for Coastal Ocean Models*. American Geophysical Union, 1995.
- [10] B.I. Dybern, D.S. Danielssen, L. Hernroth, and E. Svendsen. The Skagerrak Experiment-Skagex report 1988-1994. Technical Report 635, TemaNord 1994:635, 1994.
- [11] L.I. Eide, M. Reistad, and J. Guddal. Database av beregnede vind og bølgeparametre for Nordsjøen, Norskehavet og barentshavet, 1985. DNMI rapport.

- [12] T. Eldevik and K.B. Dysthe. Short frontal waves: May frontal instabilities generate small scale spiral eddies?, 1998. Manuscript, Department of Mathematics, University of Bergen.
- [13] H. Engedahl, B. Ådlandsvik, and E.A. Martinsen. Production of monthly mean climatological archives of salinity, temperature, current and sea level for the Nordic Seas. *J. Mar. Syst.*, 14:1–26, 1998.
- [14] R.A. Flather, R. Proctor, and J. Wolf. Oceanographic forecast models. In D.G. Farmer and M.J. Rycroft, editors, *Computer modelling in the environmental sciences*, pages 15–30. Clarendon Press, 1991.
- [15] B. Galperin, L.H. Kantha, S. Hassid, and A. Rosati. A quasi-equilibrium turbulent energy model for geophysical flows. *J. Atmos. Sci.*, 45:55–62, 1988.
- [16] D.R. Lynch, J.T.C. Ip, C.E. Naimie, and F.E. Werner. Convergence studies of tidally-rectified circulation on Georges Bank. In D.R. Lynch and A.M. Davies, editors, *Quantitative Skill Assessment for Coastal Ocean Models*. American Geophysical Union, 1995.
- [17] E.A. Martinsen and H. Engedahl. Implementation and testing of a lateral boundary scheme as an open boundary condition in a barotropic ocean model. *Coastal Engineering*, 11:603–627, 1987.
- [18] G.L. Mellor and T. Yamada. Development of a turbulence closure model for geophysical fluid problems. *Rev. Geophys. Space Phys.*, 20:851–875, 1982.
- [19] N.A. Phillips. A coordinate system having some special advantages for numerical forecasting. *J. of Meteorology*, 14:184–185, 1957.
- [20] M.D. Skogen. A user's Guide to NORWECOM. The NORwegian ECOlogical Model system. Technical Report 6, Institute of Marine Research, 1993.
- [21] D. Slagstad. A 4-dimensional physical model of the Barents Sea. Technical Report STF48 F87013, SINTEF, 1987.
- [22] J. Smagorinsky. General circulation experiments with the primitive equations, I. The basic experiment. *Mon. Weather Rev.*, 91:99–164, 1963.
- [23] J.A. Smith, P.E. Damm, M.D. Skogen, R.A. Flather, and J. Päscht. An investigation into the variability of circulation and transport on the North-West European shelf using three hydrodynamic models. *Deutsche Hydrographische Zeitschrift*, 48:325–348, 1996.

- [24] A. Stigebrandt. Barotropic and baroclinic response of a semi-enclosed basin to barotropic forcing of the sea. In H.J. Freeland, D.M. Farmer, and C.D. Levings, editors, *Proceeding of the NATO Conference on Fjord Oceanography*. Plenum Press, New York, 1980.
- [25] E. Svendsen, J. Berntsen, M. Skogen, B. Ådlandsvik, and E. Martinsen. Model simulation of the Skagerrak circulation and hydrography during SK-AGEX. *Journal of Marine Systems*, 8:219–236, 1996.
- [26] P.K. Sweby. High resolution schemes using flux limiters for hyperbolic conservation laws. *SIAM J. Numer. Anal.*, 21:995–1011, 1984.
- [27] UNESCO, 1981. Tenth report of the joint panel on oceanographic tables and standards. UNESCO Technical Papers in Marine Sci. No. 36. UNESCO, Paris.
- [28] D.-P. Wang. Mutual intrusion of a gravity current and density front formation. *J. Phys. Oceanogr.*, 14:1191–1199, 1984.
- [29] G. Weatherly and P.J. Martin. On the structure and dynamics of the ocean bottom boundary. *J. Phys. Oceanogr.*, 8:557–570, 1978.
- [30] H.Q. Yang and A.J. Przekwas. A comparative study of advanced shock-capturing schemes applied to burgers equation. *J. Comp. Phys.*, 102:139–159, 1992.